Nanoscale

ROYAL SOCIETY OF CHEMISTRY

REVIEW

View Article Online
View Journal | View Issue

Cite this: *Nanoscale*, 2025, **17**, 11191

Nanogold-albumin conjugates: transformative approaches for next-generation cancer therapy and diagnostics

Namita Jaiswal,[a,b] Nibedita Mahata[b] and Nripen Chanda *[a]

Nanogold-albumin conjugates have garnered significant attention as a highly adaptable theranostic platform, capable of delivering a wide range of therapeutics, from small-molecule drugs to larger biomolecules, while offering promising applications for monitoring and managing cancer. The remarkable theranostic capabilities of these conjugates stem from the combined strengths of gold and albumin, which provide low toxicity, a large surface area, customizable surface chemistry, and unique optical properties, all contributing to their potential in cancer therapy. This review delves into the design and development of two primary types of nanogold-albumin conjugate: supramolecular albumin-coated gold nanoparticles (GNP-BSA/HSA) and albumin-templated ultra-small gold nanoclusters (GNC-BSA/HSA). Each strategy offers distinct advantages, enabling the fine-tuning of conjugate properties to optimize therapeutic delivery and facilitate cancer-specific bio-sensing. The integration of gold and albumin further improves biocompatibility, extends circulation time, and enhances tumor targeting, making these conjugates an attractive option for cancer treatment. The review also focuses on the refinement of surface chemistry to achieve precise targeting of cancer cells, as well as the challenges and future prospects for advancing nanogold-albumin systems in clinical applications.

Received 14th December 2024,
Accepted 13th March 2025

DOI: 10.1039/d4nr05279j

rsc.li/nanoscale

1 Introduction

Cancer remains a global concern, with ever-increasing incidence and mortality rates worldwide, leading to approximately 10 million deaths annually.[1] India ranks third globally for cancer cases after China and the United States, with

[a]*Human Centered Robotics and Cybernetics Group, CSIR-Central Mechanical Engineering Research Institute, Durgapur, India. E-mail: n_chanda@cmeri.res.in*
[b]*Department of Biotechnology, National Institute of Technology (NIT), Durgapur, India*

Namita Jaiswal

Dr Namita Jaiswal is currently a Research Associate at the CSIR-Central Mechanical Engineering Research Institute (CMERI), Durgapur. She obtained her PhD from the National Institute of Technology (NIT), Durgapur, in January 2025, where her research focused on engineering nanogold-albumin conjugates for targeted cancer therapeutics. Her research interests broadly encompass nanobiotechnology, particularly in the development of delivery systems for drugs and biologics. Dr Jaiswal has authored over 15 research articles and contributed a book chapter.

Nibedita Mahata

Dr Nibedita Mahata is currently an Assistant Professor at the National Institute of Technology (NIT), Durgapur. She completed her PhD at Jadavpur University. Dr Mahata's research interest is in cell signalling, protein engineering, and developing drug delivery systems. She has published more than 30 research articles.

GLOBOCAN predicting a 57.5% increase to 2.08 million cases by 2040 from 2020.[2] Conventional chemotherapy employs a diverse array of small-molecule drugs—such as alkylating agents, anthracyclines, antimetabolites, platinum-based compounds, and various inhibitors for microtubules, topoisomerases, tyrosine kinases, and histone deacetylases—administered systemically to reach effective toxic levels. However, because these molecules are typically very small (usually under 5 nm), they are rapidly eliminated by the kidneys, which limits their presence in the bloodstream and shortens their circulation lifetime. The absence of targeting ability confers on them an undesirable bio-distribution, resulting in generic cytotoxicity to both tumor and healthy cells.[3] Moreover, prolonged exposure to such agents drives rapid cellular reprogramming, including overexpression of drug efflux transporters and the development of multidrug resistance (MDR), which ultimately contributes to treatment failure in about 90% of cases.[4] To advance oncology strategies for early diagnosis, improved therapeutic efficacy, reduced toxicity, and enhanced patient compliance, a key focus is the precise delivery of therapeutic agents to tumor cells while minimizing off-target distribution to healthy tissues. To this end, an integrated effort of interdisciplinary collaboration across engineering, physics, chemistry, biology, and medicine has been pursued over the past several decades. These collaborative efforts have led to rapid advancements in cancer nanomedicine research to overcome the constraints of conventional chemotherapy[5]—ranging from broad challenges like bio-distribution to more specific small-scale barriers, which can be mitigated by employing cell-specific targeting, molecular transport to particular organelles, and other innovative approaches.

Nanotechnology plays a crucial role in this context, encompassing the development of multifunctional nanomaterials capable of diagnosis and imaging,[6,7] targeted therapy,[8,9] controlled drug release,[10] reduced renal clearance and prolonged blood circulation,[11] improved bioavailability, and precision medicine.[12] Nanoparticles spanning a size spectrum from 1 to 1000 nm exhibit unique characteristics that enhance the effectiveness of anticancer drugs while minimizing adverse effects. Their comparable size enables them to readily interact with proteins (~1–20 nm), cell surface receptors (~10 nm), and nucleic acids (~2 nm), which in turn modify drug pharmacokinetics and promote preferential accumulation in tumors through the enhanced permeability and retention (EPR) effect.[13,14] A diverse array of nanostructures, encompassing biomolecule-based entities like liposomes,[15] various polymeric nanoparticles,[16,17] protein constructs,[18,19] ribonucleic acid (RNA) nanoparticles,[20] organic carbon-based nanoparticles (such as carbon dots,[21] nanodiamonds,[22] carbon nanotubes,[23,24] and graphene[25,26]), as well as inorganic nanomaterials made of gold,[7,27,28] mesoporous silica, superparamagnetic iron oxide,[29] and quantum dots,[30] has shown promising results in cancer therapy[6] (Table 1). However, the properties of nanostructures undergo radical changes upon entering the body due to interactions occurring at the nano–bio interface *in vivo*, leading to instabilities like particle aggregation, decomposition, and loss of functionality, which significantly affect delivery efficiency and safety.[31] Additionally, contact with physiological fluids leads to biomolecule adsorption and protein corona formation and subsequent loss of their original "synthetic identity" and the acquisition of a new "biological identity", a significant bottleneck in their successful clinical translation.[32,33] Efforts have been made to control the formation of protein coronas on nanoparticle surfaces by altering them with substances such as polyethylene glycol (PEG), carbohydrates, zwitterions, and proteins to enhance colloidal stability and prolong the circulation time in the blood.[34–36] Despite these attempts, strategies aimed at conferring targeting specificity remain challenging, as the attachment of targeting ligands to nanocarriers tends to increase the likelihood of corona formation. Consequently, this accounts for the complete loss of their integrity and the failure of numerous nanoparticle-based drug delivery systems in clinical trials.[37–41]

In this context, gold nanoparticles possess precisely regulated geometrical, optical, and surface chemical properties, which are the subject of intensive studies, as evidenced by the growing array of published research on their applications in cancer management. However, despite decades of research, only a handful of gold nanoparticles have advanced into Phase-0 (*e.g.*, AuroShell for head and neck cancers[46]) or Phase-I (*e.g.*, Aurimmune for solid tumours[44]) clinical trials for cancer therapy. This limited progress may primarily be attributed to unclear pharmacokinetics, including various aspects such as biocompatibility, bio-distribution, retention, biodegradation, excretion, and immune responses. Furthermore, the inadequate colloidal stability requires the employment of stabilizing agents like PEG, which consequently have adverse effects, including hypersensitivity resulting from complement activation and shortened bio-circulation time upon repeated dosing.[32] To overcome the pharmacokinetic limitations and improve the overall pharmacodynamics, serum albumin with a half-life of ~19 days has

Nripen Chanda

Dr Nripen Chanda is currently a Senior Principal Scientist at the CSIR – Central Mechanical Engineering Research Institute (CMERI), Durgapur, and Professor of Academy of Scientific and Innovative Research (AcSIR). He obtained his PhD from the Indian Institute of Technology Bombay and carried out his post-doctoral research at the University of Missouri-Colombia, USA. Dr Chanda's research interest is in nanomaterial synthesis, nanobiotechnology, and designing and developing micro/nanoscale devices such as sensors, actuators, drug delivery systems, and processes for interdisciplinary research in biomedical/environmental engineering. His research work resulted in seven (7) granted patents, more than 100 publications, and one (1) co-edited book.

Table 1 Overview of different nanostructures for cancer therapy and diagnostics

Nanomaterial used	Therapeutic molecule	Therapy modality	Tumour model	Status/limitations	Ref.
Pegylated liposome (Doxil)	Doxorubicin	Chemotherapy	HIV-related Kaposi sarcoma, ovarian cancer, and multiple myeloma	Approved by the FDA; approved in Europe for metastatic breast cancer	15 and 42
Liposome mifamurtide (Mepact)	Muramyl tripeptide phosphatidyl ethanolamine	Chemotherapy	Non-metastatic, resectable osteosarcoma	Approved in Europe	6 and 42
Liposomal vincristine (Marqibo)	Vincristine sulfate	Chemotherapy	Acute lymphoblastic leukaemia	Approved by the FDA	6 and 42
Polymeric methoxy-PEG-poly (D,L-lactide) paclitaxel (Genexol-PM)	Paclitaxel	Chemotherapy	Breast cancer and NSCLC	Approved in South Korea for breast cancer	6 and 42
Aminosilane-coated superparamagnetic iron oxide (SPIO) (NanoTherm)	—	Hyperthermia	Local ablation of glioblastoma multiforme; prostate and pancreatic cancers	Marketing approval in Europe for glioblastoma; Phase I/II trials in other tumor types	6 and 42
Albumin based Nab-paclitaxel (Abraxane)	Paclitaxel	Chemotherapy	Breast, lung and pancreatic cancer	Approved by the FDA	18 and 42
Pegylated liposomal cisplatin (Lipoplatin)	Cisplatin	Chemotherapy	Non-small cell lung cancer (NSCLC)	Phase III	43
Gold nanoparticle (Aurimmune, (CYT-6091))	TNF-α bound to gold nanoparticles	Photothermal ablation of tumors	Solid tumors	Phase 1	44 and 45
Gold nanoshells (AuroShell)	—	Near-infrared irradiation (NIR)	Head and neck cancer	Phase 0 (pilot study)	46
Liposomes or lipid-based NPs	Irinotecan and cisplatin	Combination of chemotherapies	*In vivo* mouse tumour models of small-cell lung cancer (SCLC)	Preclinical study	47
Poly(lactic-*co*-glycolic acid) NPs	6-Thioguanine	Chemotherapy	HeLa cells	Preclinical study	16 and 17
Carbon nanotubes	Paclitaxel	Chemotherapy	Murine 4T1 breast cancer model	Preclinical study	23
Carbon nanotubes	siRNA	Combination of hyperthermia and RNAi therapy	*In vivo* mouse tumour models of prostate cancer	Preclinical study	24
Graphene nanodots	—	Phototherapy and imaging	MDA-MB231 cancer cells	Preclinical study	25
Iron oxide NPs	Doxorubicin and curcumin	Combination of chemotherapies	*In vivo* mouse tumour models of glioma	Preclinical study	48
Gold nanorods	Doxorubicin	Combination of hyperthermia and chemotherapy	*In vivo* mouse tumour models of cervical cancer (HeLa) or KB cells	Preclinical study	49

garnered significant attention owing to its outstanding properties, including superior biocompatibility, biodegradability, non-immunogenicity, higher drug loading capacity, extended circulation lifetime, and safety for its clinical applications.[50,51]

A notable example of albumin-based nanotechnology in cancer therapy is Nab-paclitaxel (Abraxane), a first-line paclitaxel (PTX)-loaded albumin nanoformulation-based anti-cancer drug, which has been approved by the US Food and Drug Administration (FDA) for the treatment of several different cancers.[50,51] Building on this success, nanogold-albumin conjugates that synergistically combine the unique properties of gold nanoparticles and albumin have garnered significant attention as a hybrid platform for the systematic development of novel cancer therapeutic modalities.[33,52] The development of nanogold-albumin for cancer therapeutics primarily follows two key strategies: (1) the supramolecular coating of gold nanoparticles with albumin *via* active or passive adsorption (GNP-BSA/HSA) and (2) the utilization of albumin as a biological template for the *in situ* synthesis of ultrasmall gold nanoclusters (GNC-BSA/HSA). These hybrid nanostructures leverage the optical, electronic, and biocompatible features of gold with the natural bioavailability, stability, longer circulation time and drug-binding capabilities of albumin. The integration of these two components in nanogold-albumin conjugates offers several benefits, including enhanced drug loading efficiency, improved target specificity through active and passive targeting mechanisms, and reduced systemic toxicity. The protein coating also mitigates potential immunogenicity and facilitates receptor-mediated uptake in tumors or diseased tissues, making these conjugates particularly valuable in cancer therapy and other precision medicine applications. Ongoing research highlights their utility across a wide range of biomedical applications including vehicles for drug delivery,[53] gene editing, protein delivery,[54] immunotherapy, metabolism targeting,[55,56] photothermal and photodynamic therapy,[7] radiation and electromagnetic therapy, imaging and theranostic applications, and many more[52] (Fig. 1). The ability to functionalize their surfaces further expands their applicability, enabling the conjugates to be tailored for specific therapeutic or diagnostic purposes. Like albumin, the unique combinations of nanogold with other proteins are extensively explored as a versatile tool in advancing modern cancer nanomedicine (Table 2).

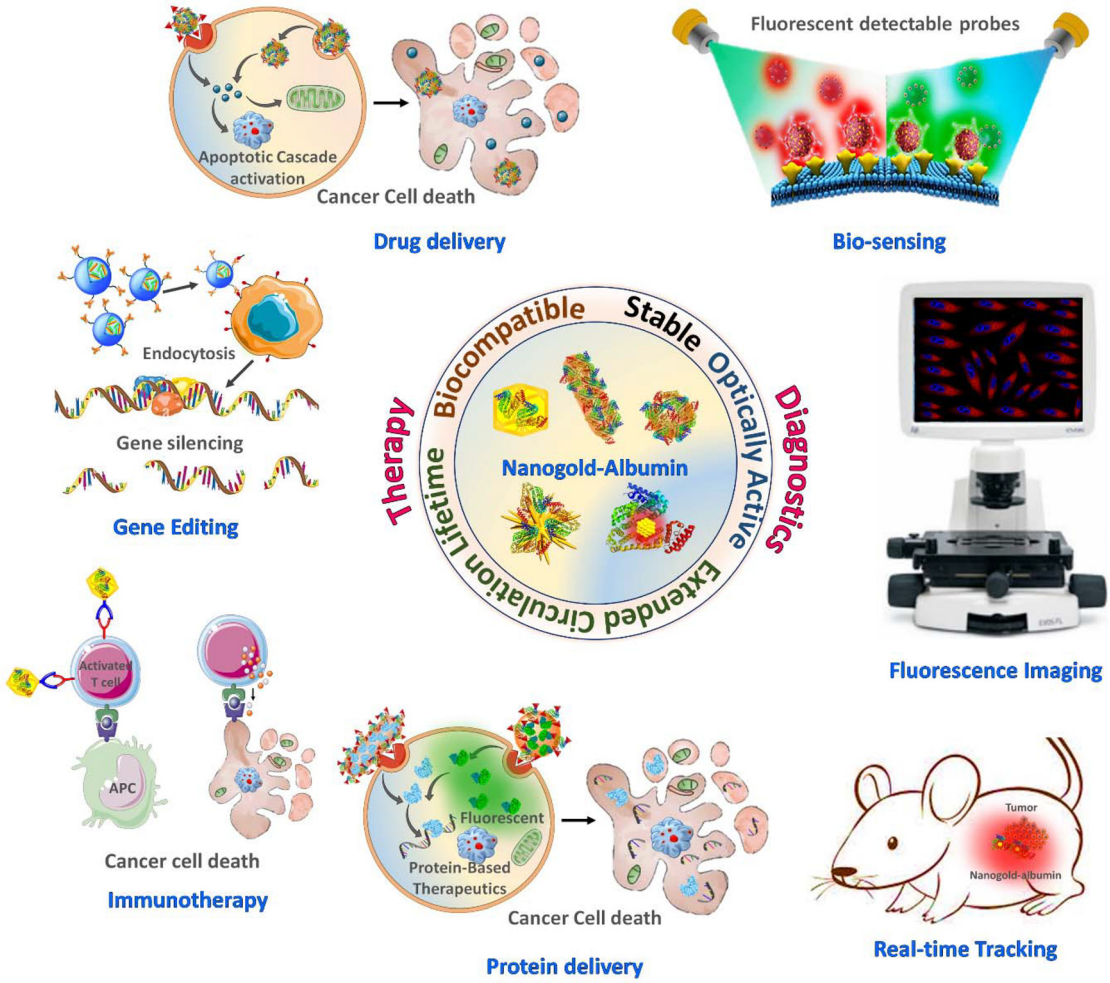

Fig. 1 Schematic illustration of nanogold-albumin conjugates for application in next-generation cancer therapy and diagnostics. Portions of this figure have been adapted/reproduced from Choi *et al.* with permission from RSC, Copyright © 2015 and Wu *et al.* with permission from Elsevier, Copyright © 2022. Portions of this figure were also produced using Servier Medical Art (https://smart.servier.com). Servier Medical Art by Servier is licensed under a CC BY 4.0 Licence (https://creativecommons.org/licenses/by/4.0/).

This review highlights recent advancements in the development of nanogold-albumin conjugates for the delivery of small-molecule drugs, proteins, and other biologics aimed at achieving tumor-suppressive effects. By offering a comprehensive overview of the current research landscape, this work aims to provide critical insights that support the rational design and clinical translation of nanogold-albumin platforms, ultimately advancing their application in enhancing cancer therapeutics.

2 Synthesis and unique properties of nanogold-albumin conjugates toward cancer management

The synthetic techniques employed for formulation of nanogold-albumin conjugates are dictated by their intended application and the specific drug molecules or biologics they are designed to encapsulate. Several established and advanced fabrication techniques, including passive adsorption, active adsorption, self-assembly, desolvation and cross-linking, emulsification and thermal gelation have been explored for the development of nanogold-albumin systems. Each of these methods is based on fundamental chemical and physical principles and offers distinct advantages in optimizing nanoparticle size, morphology, colloidal stability, encapsulation efficiency and surface characteristics for efficient loading, and release behaviour. Owing to the integrated properties of gold and albumin, the nanogold-albumin-derived structures exhibit variations in size, shape, biophysical and optical properties, and biocompatibility. These platforms further benefit from albumin's ability to interact with receptors overexpressed in many diseased tissues and cells, enabling targeted delivery to disease sites without requiring additional specific ligands.[19] Different methods of nanogold-albumin synthesis are discussed in subsequent sections.

2.1 Synthesis techniques of nanogold-albumin conjugates

The existing synthesis methodologies can broadly be classified into two categories: (1) supramolecular coating of gold nano-

Table 2 Overview of different protein-based nanoparticle composites for cancer therapy and diagnostics

Nanomaterial used	Protein/drug/targeting agent	Therapy/diagnostics	Tumour model/s	Remarks/limitations	Ref.
Gold nanoparticles	Anti-epidermal growth factor receptor (anti-EGFR) antibodies for targeting	SPR-based imaging diagnosis of oral epithelial living cancer cells *in vivo* and *in vitro*	HOC 313 clone 8 and HSC 3 cells	Specific binding to the cancerous cells with six times greater affinity than the noncancerous cells; impact of nanoparticles on the tumor immune microenvironment needs to be studied.	57
Gold nanorods	Mouse serum, chlorin e6 (Ce6)	Combination of PDT and PTT therapy	OSCC cells, female NCr OSCC xenograft nude mice	Significant PTT heating-induced tumor ablation, coupled with PDT-induced cell killing by oxidative stress, and subsequently complete tumor elimination with no regrowth; only short-term biocompatibility studies were conducted.	58
Gold nanorods	CRISPR/Cas9-ribonucleoprotein, nuclear targeting peptide (TAT) for targeting	Combination of targeted gene editing and PTT therapy	MCF-7 cells	Enhanced antitumor effect through the combination of gene editing from the loaded sgRNA/Cas9 complex and photothermal effect from gold nanorods; further studies are needed on biological performance, stability, and bio-distribution *in vivo.*	59
Gold nanorods	Apolipoprotein E, chlorin e6 (Ce6)	Combination of PTT and PDT therapy	Cal 27 cells	Enhanced death in Cal 27 cells and increased intracellular generation of ROS; the bio-distribution characteristics and therapeutic performance *in vivo* need to be evaluated.	60
Gold nanorods	Human serum, chlorin e6, doxorubicin	Multimodal cancer therapy: PDT, PTT and chemotherapy	Cal 27 cells	Enhanced uptake by Cal 27 cells followed by a near complete eradication of cancer cells; the bio-distribution characteristics and therapeutic performance *in vivo* need to be evaluated.	61
Gold nanorods	Anti-epidermal growth factor receptor (anti-EGFR) antibodies for targeting	Photoacoustic imaging (PAI)-guided near-infrared photothermal therapy	MDA-MB-231, MCF-7, BT-474 cells; female BALB/c nude mice injected with MDA-MB-231-Luc cells	Synergistic anti-proliferative and apoptotic actions in triple negative breast cancer (TNBC) through upregulation of HSP70 and cleaved caspase-3; further animal and clinical trials are required to assess distribution characteristics and safety.	62
Gold nanorods	Anti-carbonic anhydrase IX (CAIX) antibody	Photothermal therapy	HT29 cells, Swiss Nu/Nu mice were xenografted with HT29 tumors	Selective internalization in CAIX-overexpressing hypoxic cells, highly effective in eliminating cancer cells; further animal and clinical trials are required to assess safety and efficacy.	63
Gold nanoclusters	Keratin, doxorubicin	Chemotherapy, NIR fluorescence imaging, MRI	4T1 cells	Significant reduction in tumor growth, enhanced NIR fluorescence imaging, high colloid stability; studies are needed on biological performance, bio-distribution, and therapeutic performance *in vivo*.	64
Gold nanoclusters	Ribonuclease-A, vitamin B12 for targeting	Imaging and diagnostics	Caco-2 cells	Suitable for simultaneous targeting and imaging of cancer at the cellular level; detailed studies are needed on imaging and diagnostic potential *in vivo*.	65
Gold nanoclusters	Ribonuclease-A	Imaging and diagnostics	Caco-2, and HCT116 cells, C57BL/6 mice	Could successfully distinguish intestinal tumor mice from healthy mice, indicating a potential utility for early diagnosis of intestinal tumors; further clinical trials are required to assess safety and efficacy.	66

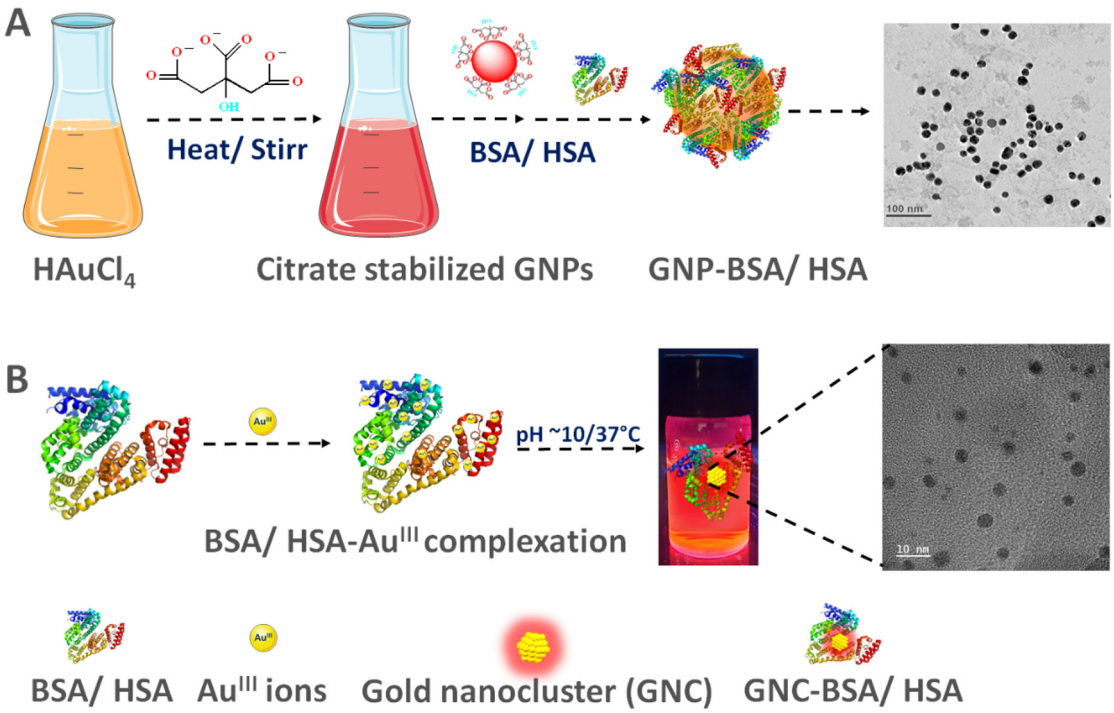

Fig. 2 Schematic for synthesis and modification of nanogold-albumin types. The development of nanogold-albumin conjugates primarily follows two strategies: (A) supramolecular coating of gold nanoparticles with albumin *via* active or passive adsorption (GNP-BSA/HSA), and (B) utilizing albumin as a template for the *in situ* synthesis of ultrasmall gold nanoclusters (GNC-BSA/HSA). This figure has been adapted/reproduced from Jaiswal *et al.* with permission from Elsevier, Copyright © 2024.[56]

particles (GNPs) with albumin *via* active or passive adsorption and (2) utilizing albumin as a template for the *in situ* synthesis of ultra-small gold nanoclusters (GNCs) (Fig. 2). Supramolecular capping of GNPs with albumin is achieved through electrostatic or hydrophobic interactions between the gold nanoparticles and albumin or through the chemisorption of thiols on the gold surface. On the other hand, the albumin-templated approach enables the formation of GNCs through either bottom-up or top-down methodologies, resulting in unique fluorescence properties driven by discrete electronic transitions distinct from those observed in GNPs.[67] The bottom-up approach, known as the atoms-to-clusters synthesis pathway, involves assembling GNCs from individual ions and atoms. In contrast, the top-down method is a traditional technique where GNPs are fabricated first and subsequently etched with excess ligands to generate GNCs.[67]

2.1.1 Supramolecular functionalization with albumin through passive adsorption. Passive adsorption represents one of the most straightforward and effective approaches for synthesizing nanogold-albumin conjugates, leveraging the natural affinity of albumin for gold surfaces. This process occurs through the interaction of charged functional groups or specific atoms within albumin with the gold nanoparticle surface, facilitated by either covalent or non-covalent interactions. Albumin, with its abundance of reactive groups such as carboxylic acids, thiols, amines, and metal-binding regions like the N-terminal amine and free cysteine (Cys-34), provides versatile interactions with GNP surfaces, making it instrumental in the creation of multifunctional nanogold-albumin platforms.[52,68] This adsorption-based method is typically accomplished through a simple incubation process, wherein a solution of GNPs is mixed with albumin, leading to spontaneous binding.[54,69] The primary advantage of this strategy lies in its methodological simplicity and cost-effectiveness, as it eliminates the need for additional reagents, chemical modifications, or extreme reaction conditions. One limitation of this strategy is that the extended shelf life of nanogold-albumin conjugates may be compromised due to the weak and reversible nature of physical adsorption. Thus, passive adsorption may serve as a widely utilized approach for fabricating biocompatible and functional nanogold-albumin conjugates, making it particularly attractive for applications in drug delivery, bio-imaging, and bio-sensing applications.

2.1.2 Supramolecular functionalization with albumin through active adsorption. Active adsorption offers a more controlled approach to synthesizing nanogold-albumin conjugates, involving the modification of albumin to enhance its binding efficiency and interaction specificity with gold nanoparticles or their functionalized surfaces. Unlike passive adsorption, this strategy involves pre-functionalization, resulting in derivatives such as carboxylated, thiolated, cationic, or anionic albumin.[70,71] These modifications improve stability, surface coverage, and compatibility with pre-functionalized GNP surfaces. This approach is particularly advantageous

when GNPs are coated with additional molecules or polymers, such as polyethylene glycol (PEG), where an albumin layer is needed to enhance biocompatibility and performance. For instance, in GNP-PEG formulations, cationic bovine serum albumin (BSA) has been shown to improve the stability and uniformity of the coating. The ability to tune the electrostatic and chemical interactions between albumin and GNPs through functionalization makes active adsorption a valuable technique for applications requiring precise surface engineering, such as targeted drug delivery, bio-imaging, and theranostics for cancer management.[72]

2.1.3 Albumin-templated *in situ* synthesis through a bottom-up approach. The bottom-up approach, also referred to as the atoms-to-clusters synthesis route, involves the formation of nanoclusters (GNCs) from individual atoms and ions. This method enables the controlled assembly of GNCs from precursor metal ions in a stepwise manner. In this strategy, albumin is incorporated during the synthesis process, acting as a reducing and stabilizing agent to facilitate the formation of biocompatible ultra-small GNCs, which offer enhanced stability, solubility, and surface functionality.[73–75] Notably, Xie *et al.* pioneered a simple, one-pot, and environmentally friendly synthesis strategy to generate highly luminescent BSA-Au_{25} nanoclusters directly from Au^{3+} ions in aqueous conditions, without requiring an additional reducing agent.[73] This innovative approach highlights the potential of albumin-assisted synthesis for producing biocompatible gold nanoclusters with unique optical and chemical properties.

Furthermore, recent advancements in nanogold-albumin conjugate synthesis have focused on rapid, eco-friendly methodologies that enhance efficiency and control over nanoparticle formation. One such approach involves microwave (MW) irradiation, which significantly accelerates the synthesis of bovine serum albumin-gold nanoclusters (GNC-BSA), reducing the reaction time from several hours to just a few minutes.[67] Yan *et al.* demonstrated the MW-assisted synthesis of red-emitting GNC-BSA, wherein a BSA solution was mixed with an Au^{3+} salt solution, followed by NaOH addition and MW irradiation for 6 minutes. This process resulted in a colour change from light yellow to dark brown, indicating successful nanocluster formation.[76]

Alternatively, ultrasonic irradiation, or sonochemical synthesis, has been explored as a rapid method for fabricating GNC-BSA with near-infrared (NIR) emission. Liu *et al.* introduced this approach by adding an aqueous Au^{3+} solution to a BSA solution, adjusting the pH to 12, and subjecting the mixture to ultrasonic irradiation under ambient conditions, producing a light brown colloidal solution.[77] More recently, a photocatalytic strategy has been employed for the controlled synthesis of GNC-BSA with tunable fluorescence.[78] In this method, silver nanoclusters were initially generated *via* UV light-induced reduction of silver ions. These pre-formed silver nanoclusters subsequently facilitated the reduction of $HAuCl_4$ to GNCs, which were stabilized within BSA molecules. The resulting fluorescence emission of the GNC-BSA was adjustable, ranging from 570 to 620 nm, depending on the synthesis conditions. These innovative approaches demonstrate the potential for the rapid, scalable, and environmentally friendly synthesis of nanogold-albumin conjugates, making them promising candidates for biomedical applications such as drug delivery, bioimaging, and theranostics.

2.1.4 Albumin-templated *in situ* synthesis through a top-down approach. The top-down approach is a widely employed method for fabricating nanomaterials, involving the size reduction of larger gold nanoparticles (GNPs) through controlled etching processes to generate gold nanoclusters (GNCs). This core-etching strategy is commonly used for synthesizing gold (Au) and silver (Ag) nanoclusters, where excess ligands—such as dihydrolipoic acid (DHLA), mercaptoundecanoic acid (MUA), and glutathione (GSH)—facilitate the breakdown of larger nanoparticles over an extended reaction period.[67] In some cases, external stimuli such as heat or pH adjustments are applied to accelerate the etching process and enhance the yield of smaller nanoclusters.

Pradeep *et al.* reported the use of bovine serum albumin (BSA) as an etching ligand to synthesize red-fluorescent GNC-BSA.[79] Initially, mercaptosuccinic acid (MSA)-stabilized GNPs were synthesized, which then underwent BSA-mediated core etching under alkaline conditions (pH 12). This process resulted in GNC-BSA consisting of 38 Au atoms (Au_{38}) with a photoluminescence quantum yield of approximately 4%. The reaction progress was monitored by tracking the gradual increase in photoluminescence (PL) intensity, corresponding to the formation of smaller, highly fluorescent nanoclusters. Despite its widespread application in the synthesis of ligand-capped GNCs, the top-down approach remains underexplored for protein-based nanoclusters. This limitation arises from the harsh chemical conditions required for core-etching, which can destabilize proteins, leading to structural denaturation and broad size distributions in the resulting nanoclusters. Further research is needed to elucidate the dynamics of nanocluster formation *via* this method and to optimize BSA-mediated etching strategies, ensuring higher stability and uniformity of the protein-stabilized gold nanoclusters.

2.1.5 Desolvation and cross-linking approach. The desolvation and cross-linking method, also referred to as the coacervation process, is a widely employed technique for fabricating core–shell albumin-gold nanoparticles. In this approach, GNPs are introduced into a albumin solution, where they act as nucleation sites for nanocapsule formation. Subsequently, an organic solvent—typically methanol, ethanol, or acetone—is gradually added dropwise until a turbid suspension is formed, indicating the desolvation of albumin. This process significantly reduces the water solubility of albumin, leading to phase separation and the formation of protein aggregates. Upon desolvation, amine groups on the albumin molecules become exposed, enabling cross-linking *via* chemical agents such as glutaraldehyde, which stabilizes the nanostructure. This method offers a key advantage in nanogold-albumin conjugate synthesis, as it facilitates the physical encapsulation of various bioactive agents—including nanoparticles, pharmaceuticals, and diagnostic molecules—within the nanogold-

albumin matrix. The resulting nanocapsules exhibit high stability, effectively shielding their encapsulated components from degradation, thereby enhancing their therapeutic and diagnostic potential.[52,80,81]

2.1.6 Emulsification-based synthesis. The emulsification technique is an effective approach for synthesizing nanogold-albumin conjugates, leveraging the hydrophobic amino acids present in albumin. In this process, an albumin solution is combined with a non-aqueous phase (oil) and subjected to shear mixing or high-pressure homogenization, leading to the formation of a stable emulsion. This method enables the incorporation of GNPs functionalized with hydrophobic molecules, which serve as nucleation sites, facilitating interactions with the hydrophobic residues of albumin and forming a core–shell structure.[70] To ensure the stability of the resulting nanocapsules, either chemical cross-linking agents or high-temperature stirring can be employed. The final step involves solvent removal through low-pressure evaporation, yielding well-defined nanogold-albumin structures. This emulsification strategy is particularly advantageous for encapsulating lipophilic drugs, enhancing their biocompatibility and aqueous solubility, making it a valuable technique for drug delivery applications.[52,82]

2.1.7 Thermal gelation-based synthesis. The thermal gelation method utilizes temperature-induced protein unfolding to facilitate the formation of nanogold-albumin conjugates. Since albumin is highly responsive to temperature changes, heating its aqueous solution causes the disruption of its native structure, exposing hydrophobic, electrostatic, disulfide, and hydrogen bonding sites. This structural rearrangement promotes protein–protein interactions, leading to the formation of a gel-like network. Additionally, the unfolding of albumin enhances its affinity for GNPs, enabling self-assembly onto the GNP surface. This results in the formation of a stable protein coating, which can enhance nanoparticle stability, functionality, and biocompatibility. The thermal gelation approach offers a simple and effective method for fabricating nanogold-albumin systems, making it particularly useful for biomedical applications such as drug delivery, bio-imaging and biosensing.[52,82]

2.2 Bio-physico-chemical properties

The physico-chemical characteristics of nanoparticles, such as size, shape, chemical composition, crystal structure, surface area, surface energy, surface roughness, and stability, impact the unique properties of nanostructures, which in turn play a crucial role in determining their effectiveness as drug delivery and theranostics platforms. The rapid advancement of synthetic procedures has enabled precise control over these properties, allowing the fabrication of nanogold-albumin conjugates with customizable attributes even in basic laboratory setups. By employing GNPs of different shapes—such as nanospheres, nanorods, nanocages, nanoshells, nanostars, nanoprisms, nanovesicles, nanoflowers, nanocubes, and ultrasmall nanoclusters (GNCs)—researchers can tailor the properties and functionalities of nanogold-albumin conjugates to address specific biomedical needs.[28] These diverse geometries influence the biophysical interactions at the nano–bio interface, and a precise understanding of these interactions is helpful for drug encapsulation, specific targeting, stimulus-responsive drug delivery, theranostics, and enzymatic mimetic applications.[72,83]

2.2.1 Analytical studies. GNPs are efficient adsorbents of BSA molecules in an aqueous solution, with the adsorption being influenced by contact time, initial BSA concentration, and temperature. It is reported that adsorption increases with time, peaking at 20 minutes. An increase in pH to around 8.6 also increases the adsorption of BSA on GNPs. High BSA concentration and pH enhance adsorption, while high temperature reduces it, indicating an exothermic and chemisorptive process.[71] Nanogold-albumin, especially that prepared with gold nanospheres and nanorods, displays differential interaction behaviour with bovine serum albumin (BSA). The complexation of BSA with nanospheres is primarily enthalpy-driven (exothermic in nature), where the native structure and properties of BSA are retained. In contrast, the complexation of BSA with nanorods is entropically driven, followed by the substantial loss in protein secondary and tertiary structures with the release of a large amount of bound water. Nanogold-albumin derived from nanorods and nanospheres stabilized with BSA has been reported to show static fluorescence quenching, probably due to the alterations in the microenvironment near the tryptophan and tyrosine amino acid residues of BSA and HSA.[84,85] Furthermore, the size of GNPs also governs their interaction with albumin. GNPs of size ~8 nm are found to quench the fluorescence of BSA more efficiently, primarily due to the increased surface area resulting from the reduction in particle size. Moreover, binding constants are higher with smaller particles, indicating the adsorption of a greater number of BSA molecules per unit area of the GNP surface.[86] Shang *et al.* reported that nanogold-albumin, prepared through nano-spheres and BSA following standard adsorption methods at pH 3.8, 7.0, and 9.0, resulted in substantial conformational changes of albumin at both the secondary and tertiary structure levels. Higher pH resulted in a greater decrease in α-helical content, possibly originating from the intrinsic conformational state of BSA adopted at different pH values.[87,88] Strozyk *et al.* demonstrated that citrate or cetyltrimethylammonium bromide (CTAB) stabilized nanospheres, when capped with BSA, showed exceptional colloidal stability under physiological conditions and exhibited reversible U-shaped pH-responsive behaviour similar to pure BSA.[89]

The nanogold-albumin platform offers versatile surface chemistry, combining the functional attributes of the GNP core with the albumin's surface, comprising both hydrophobic and hydrophilic domains and abundant charged amino acids. This provides numerous chemically active groups for surface functionalization for anchoring targeting moieties and also serves as a platform for loading drug molecules for cancer therapy.[19] In a recent study by Jaiswal *et al.*, a ground state complex formation was reported between cisplatin (CPT) bound BSA and GNP. Spectroscopic analysis revealed a stron-

ger binding affinity of the BSA-CPT conjugate to GNP compared with BSA alone, indicating a greater apparent association constant, suggesting CPT-induced conformational changes in the BSA, leading to stronger adsorption of the BSA-CPT conjugate onto GNP.[90]

By altering the synthesis parameters to alkaline conditions (pH ~12), albumin serves as a template for synthesizing fluorescent quantum-sized nanogold-albumin conjugates (GNC-BSA, typically below 2 nm).[67] Recent research by Zhong *et al.* highlights the strong correlation between the ultrasmall size and size-tunable physicochemical properties of fluorescent GNC-BSA and the number of charged groups on the BSA surface.[91] To achieve BSA variants with more positive net charges (cBSA, +13.9 ± 0.9 mV) and more negative charges (aBSA, −31.4 ± 1.2 mV), ethylenediamine and succinic anhydride are employed to react with the carboxyl and amino groups of BSA (nBSA, −9.7 ± 1.1 mV), respectively. The mean core diameters of GNC-cBSA, GNC-nBSA, and GNC-aBSA thus obtained are 1.91 ± 0.11, 2.54 ± 0.23, and 2.97 ± 0.2 nm, respectively. These differences in GNC-BSA size likely stem from variations in the number of amino groups between native and modified BSA.

2.2.2 Molecular dynamics simulation. Molecular dynamics (MD) simulations have become an invaluable tool in understanding the interaction mechanisms between nanogold-albumin conjugates and biological systems. These simulations provide atomistic-level insights into the structural and dynamic changes induced in albumin upon binding to gold nanoparticles.[92] Studies have demonstrated that GNPs alter the secondary structure and flexibility of albumin through non-bonded interactions, primarily van der Waals and electrostatic forces.[92,93] Such alterations can influence the protein's stability, conformational dynamics, and biological function, impacting drug loading and release capabilities.[92] MD simulations conducted by Kaumbekova *et al.* reveal that 5 nm GNPs, in the presence of NaCl, induced changes in the BSA secondary structure during the initial binding phase.[93] Further analysis demonstrates the effect of smaller GNPs (3 nm) and gold nanoclusters (GNCs, 1 nm) on BSA binding sites. While stable BSA-gold conjugates are observed across different nanoparticle sizes, no specific binding sites are identified. Notably, 1 nm GNCs cause a greater degree of protein unfolding, leading to a significant reduction in helical content and hydrogen bonding, demonstrating the size-dependent impact of GNPs on protein conformation.

The influence of nanoparticle shape on albumin interactions has also been explored through MD simulations. Studies comparing the binding of nanocubes and nanospheres with HSA showed that nanocubes induce greater protein unfolding compared with nanospheres. These interactions alter albumin angles and bond lengths, with nanocube interactions significantly modifying the helix length and polarity, while nanosphere interactions predominantly affect the psi (Ψ) and phi (Φ) angles.[94] Ramezani *et al.* investigated the docking interactions between HSA and GNPs, employing MD simulations and the GOLP force field to analyze protein structural changes.[95] Their findings demonstrate that HSA undergoes denaturation upon GNP adsorption, with a marked decrease in alpha-helix content. Domain III, known for its fatty acid binding sites, plays a key role in the adsorption process. Critical amino acids involved in HSA-GNP interactions include Lys464, Thr504, Phe505, and Leu581. Additionally, increased fluctuations in certain protein domains indicate structural destabilization following nanoparticle adsorption.

In another significant study, Rajan *et al.* examined the binding interactions of BSA and HSA with gold nanorods (AuNRs) to determine the nature and extent of contact between serum albumins and nanorod surfaces.[84] Computational studies revealed that the planar surface of AuNRs interacts with cysteine (Cys) residues (Cys-316 and Cys-368) from BSA and HSA, forming Au–thiol coordination bonds with bond lengths of 3.722 Å and 3.442 Å, respectively. The presence of a sulfide linkage facilitates stable nanogold-albumin conjugate formation, as confirmed by MD simulation results, indicating high stability and strong protein–nanoparticle interactions. These molecular simulation findings collectively highlight the significant role of nanoparticle size, shape, and surface chemistry in determining albumin conformational stability and interaction dynamics, which is indispensable for predicting protein corona formation, assessing drug delivery potential, and optimizing the nanogold-albumin conjugates for biomedical applications.

2.3 Optical properties

The optical properties of gold nanoparticles (GNPs) differ markedly from those of bulk gold due to variations in electron behaviour at the nanoscale. While bulk gold exhibits a characteristic yellow colour, GNPs in solution display a striking red appearance.[67,96] In bulk gold, the energy levels of electrons are compressed, forming a continuous spectrum without a clear band gap between the valence and conduction bands. However, GNPs, typically sized between 2–100 nm, are comparable to, or smaller than, the mean free path of electrons, facilitating interactions with electromagnetic waves and leading to collective oscillations of surface electrons – a phenomenon famously referred to as the surface plasmon resonance (SPR) effect. The SPR is the source of the ruby red colour of conventional GNPs.[97] The dependence of the resonant wavelength on the nanostructures' size, shape, and geometry provides opportunities to manipulate the optical properties as needed.

In nanogold-albumin conjugates, the optical properties are closely related to their structures, including the morphology of the nanostructures and the molecular interactions present. For instance, the different structures of GNPs (sphere, rod, shell, cage, star, flower), together with the nature of the chemical interaction between GNPs and albumin (adsorption or covalent binding), contribute to the unique optical properties and characteristics of nanogold-albumin, which further decide their subsequent applications in imaging, therapy, and theranostics (Table 3).[96] The variation in SPR absorbance in nanogold-albumin conjugates might arise due to the subtle differences in surface electrostatic interactions and structural differ-

Table 3 Optical properties of different types of nanogold-albumin conjugate

Type of nanogold-albumin NP	Mechanism of interaction	UV-Visible		Fluorescence				Ref.
		λ_{max} (nm)	Shift (nm)	λ_{ex} (nm)	λ_{em} (nm)	Lifetime (ns)	QY (%)	
GNP-BSA_{FA}-EGFP GNP-BSA_{FA}-RNaseA	Hydrophobic	λ_T = 510 λ_L = 819	λ_L = 846 λ_L = 842	—	—	—	—	54
GNC-BSA-TG	Hydrophobic, hydrogen bonding, Au–S interaction	—	—	520	645	—	—	56
GNP-HSA, GNP-BSA	Hydrophobic	λ_T = 521	λ_T = 524 λ_T = 522	—	—	—	—	98
GNC-BSA (Au_{25})	Au–S bonding	—	—	480	640	—	6	73
GNC-BSA (Au_{16})	Au–S bonding	—	—	500	608	170	—	102
GNC-BSA (Au_8), GNC-BSA (Au_{25})	Au–S bonding	—	—	370 370, 530	450 685	0.8 ± 0.2 3.0 ± 0.3 1.78 ± 0.3 184 ± 7.0	6.07 5.53	103
GNC-BSA (Au_{25})	Au–S bonding	—	—	470	660	1880 440 9	~6	104
GNC-cBSA, GNC-nBSA, GNC-aBSA	Au–S bonding	—	—	500	673 684 691	2150 1930 1820	—	91
GNC-BSA-FA	Au–S bonding	—	—	530, 569	674	—	5.7	105

ences of albumin from different sources.[51] Furthermore, albumins, such as ovalbumin, bovine serum albumin (BSA), or human serum albumin (HSA), vary in molecular weight, size, structure, S–S bridges, and SH groups. These variations significantly affect the binding abilities, surface modifications, and the formation of nanogold-albumin conjugates.[51] Of note, the optical properties of nanogold-albumin could easily be tailored for the desired absorption/scattering ratios and wavelengths based on the sizes and shapes of the GNPs used for synthesis. For instance, HSA-conjugated GNPs show increased SPR absorbance with a 2–3 nm red shift, while the BSA-conjugated ones attenuate slightly with a 1 nm red shift and broader baseline.[98] A change in pH from alkaline to acidic results in a broadening and red shift of the SPR band for the BSA-conjugated gold nanospheres.[87] Interestingly, BSA-stabilized gold nanorods exhibit optical and colloidal properties similar to the CTAB-stabilized ones with no significant changes in their LSPRs characteristic peaks.[69] The absorption/scattering wavelength of nanogold-albumin formed by gold nanocages or nanostars could easily be tailored by adjusting the thickness of the wall, the lengths of the outer edges of the nanocage, and the number of tips in the plane, respectively.[99]

Further reduction in the size of gold nanoparticles (GNPs) to the scale of a few to several hundred atoms—approaching the Fermi wavelength of electrons (~0.5 nm for gold)—leads to the formation of extremely small gold nanoclusters (GNCs). These GNCs typically range in size from 1–3 nm and exhibit unique, molecule-like properties due to discrete electronic transitions, in contrast to the continuous plasmonic behavior observed in larger GNPs. These quantum-sized GNCs stabilized by albumin, first reported by Xie *et al. via* a 'green' synthetic process where BSA was both a reducing agent and a stabilizer, yielded bright red-emitting GNC-BSA ($\lambda_{em\ max}$ = 640 nm) with a quantum yield (QY) of ~6%.[73] The red fluorescence of GNC-BSA stems from the 25 Au atoms (Au_{25}) stabilized by the BSA.[100] These newer nanogold-albumin conjugates exhibit remarkable photostability, biocompatibility, high emission rates, and large Stokes shifts. Their photoluminescence could be effectively tuned over broad wavelengths ranging from near-infrared (NIR) to ultraviolet (UV) regions by tuning their core size.[67] Tuning synthesis parameters is essential for controlling the number of metal atoms or ions, which in turn significantly affects the size and optical properties of gold nanoclusters (GNCs). Microwave-assisted synthesis at135 °C for 4 min results in small-sized (3.1 ± 0.4 nm) blue-emitting GNC-BSA, whereas synthesis at 80 °C for 4 min yields larger (4.2 ± 0.5 nm) red-emitting GNC-BSA.[101] This variation in synthesis temperature leads to increased luminescence intensity at 436 nm (at 135 °C) and 676 nm (at 80 °C), corresponding to red and blue GNC-BSA, respectively.[101] Notably, the optical properties of GNC-BSA are also influenced by the number of charged groups on the surface of the BSA.[91] The fluorescence emission and luminescence lifetime of GNC-BSA is highest for positively charged albumin, followed by neutral, and least for negatively charged. The findings above strongly indicate that nanogold-albumin synthesized from GNP/GNC and different albumin variants exhibits markedly different photophysical properties including size-dependent emission and surface-enhanced fluorescence, making it ideal for high-sensitivity imaging in cellular and deep-tissue applications.

2.4 Biocompatibility

Biocompatibility is the ability of a material to perform with an appropriate host response in a specific application.[106] The majority of the biocompatible nanomedicines, upon contact with physiological fluids, gets coated with various biomolecules (corona formation), making them susceptible to clearance by the mononuclear phagocytic system (MPS).[107]

The corona formation process, driven by the need to reduce energy, involves the entropy-driven displacement of water molecules, particle surface charge compensation, and shielding of hydrophobic regions. The nature of the binding proteins present in biological fluids controls the phagocytosis of nanoparticles, governing their time in the systemic circulation. Previous research suggests that the retention and biocompatibility of nanoparticles in the systemic circulation are significantly enhanced in the presence of albumin (dysopsonins protein), which inhibits the complement activation, thus reducing the susceptibility of nanoparticles to phagocytosis and prolonging the circulation time in the bloodstream. In this regard, extensive research has been undertaken to study nanogold-albumin's biocompatibility and potential toxicity by employing both *in vitro* and *in vivo* approaches.[52] Tebbe *et al.* have demonstrated that gold nanorod-BSA, synthesized after the complete replacement of CTAB with BSA in a large range of aspect ratios and sizes, is highly stable at pH values above, as well as below, the isoelectric point of BSA (pI = 4.8). These nanostructures exhibited remarkable colloidal stability in aqueous solutions at different conditions with or without 10% bovine calf serum.[69] Khullar *et al.* showed that GNP-BSA formed by unfolding BSA to passivate the GNP surface showed negligible hemolysis and cytotoxic responses to cells compared with cationic surfactant-coated GNP controls.[108] Similarly, positively charged GNP-BSA, synthesized using a green synthesis method with various diameters (80–1500 nm), was efficiently internalized by MG-63 osteosarcoma cells and showed minimal toxicity to the cells.[109] Additionally, GNP-BSA were found to exhibit high colloidal stability and extreme compatibility at high concentrations (100 μg ml^{-1}) towards normal (L929) and cancerous (KB) cells without the generation of reactive oxygen species (ROS) and hemolytic responses towards red blood cells.[110] Overall, the collective evidence suggests that nanogold-albumin exhibits diminished hemolytic activity and low toxicity, making it suitable for drug delivery applications at targeted sites.[52] Compared with *in vitro* studies, *in vivo* and *ex vivo* biocompatibility evaluation in animal models is a better measure to analyze the potential impact of nanogold-albumin platforms on human health. One notable *ex vivo* study by Mocan *et al.* focused on using GNP-BSA as an active vector to target liver cells.[111] GNP-BSA administered intra-arterially into the *ex vivo*-perfused liver specimens obtained from hepatocellular carcinoma patients showed selective accumulation of GNP-BSA punctuate structures mainly spread into the malignant tissue and most predominant inside the tumour core. Furthermore, tissue obtained from adjacent liver parenchyma was not seriously affected, indicating the biocompatibility of the nanostructures toward healthy tissues. Another notable study in mice with GNP stably conjugated with HSA (GNP-HSA) showed massively reduced liver retention (52%) compared with apolipoprotein E (GNP-apoE, 72%) or citrate-stabilized GNPs (>95%).[112] The authors also observed an increased blood circulation time of GNP-HSA. Additionally, higher retention of GNP-HSA in the lungs and brain was observed compared with GNS-apoE and citrate-stabilized GNPs. The ability of this nanogold-albumin platform to cross the blood–brain barrier and target the lungs may be beneficial in overcoming some of the existing obstacles in brain- and lung-related cancer therapies.

The interaction with the immune system presents a major challenge to the success of cancer nanomedicine, with concerns about potential toxicity, as well as the risk of triggering allergic reactions and inflammation, remaining key considerations for nanomaterials in biomedical applications. Nanogold-albumin-based carriers show promise in overcoming phagocytosis by monocytic and dendritic cells, as well as macrophages, by reducing particle adhesion to cell membranes.[32] Li *et al.* demonstrated that the dispersion and stabilization of gold nanorods coated with BSA (GNP-BSA) depends on the BSA to GNP ratio; lower ratios show agglomeration, while higher ratios support colloidal stability.[113] Interestingly, the authors observed a significantly reduced uptake of GNP-BSA (2 μg mL^{-1}) by RAW 264.7 macrophages, demonstrating the stealth effect and the potential of these nanogold-albumin platforms to escape clearance by the MPS.

3 Nanogold-albumin conjugates as delivery and imaging agents

3.1 Drug delivery: EPR effect and release mechanism

The development of next-generation nanocarriers for drug delivery relies on the selective targeting of cancer cells by overcoming the limitations of conventional delivery methods. These limitations range from large-scale challenges like biodistribution to small-scale barriers like intracellular trafficking. Critical factors, including nanoparticle size, geometry, surface charge, and modifications, are pivotal in determining their hemodynamic behaviour and interaction with the tumor microenvironment (TME). These properties influence the enhanced permeability and retention (EPR) effect, which governs the systemic delivery of drugs and subsequent therapeutic outcomes.[12] The tumour microenvironment (TME) significantly influences the fate of nanoparticles and, consequently, the efficacy of cancer nanomedicine. The hallmark features of the TME—heterogeneous and abnormally leaky vasculature—facilitate nanoparticle extravasation and preferential accumulation at tumor sites, a phenomenon known as the EPR effect.[12] Studies indicate that the neo-vascularization in cancers, defective angiogenesis, and impaired lymphatic drainage contribute to the increased retention of up to 10–15% of administered nanomedicine, compared with 0.1% of free drugs.[114] The EPR effect constitutes "passively targeted" nanoparticles relying on their nanometric size (~100 to ~200 nm) for preferential accumulation in the tumour.[115] The effectiveness of several nanoparticles currently utilized in clinical settings, such as Doxil™, Abraxane™, Marqibo™, DaunoXome™, and Onivyde™ in the US; Myocet™ and Mepact™ in Europe; Genexol-PM™ in Korea; and SMANCS™ in Japan, provides additional evidence supporting the significance of the EPR effect in cancer nanomedicine.[116]

However, interpreting EPR as a product of leaky tumour vasculature and poor lymphatic drainage in complex biological systems may be an oversimplified interpretation. The systemic administration of nanoparticles must navigate multiple physiological barriers, including nanoparticle-protein interactions, blood circulation dynamics, clearance by the mononuclear phagocyte system (MPS) or reticuloendothelial system (RES), extravasation into the perivascular tumor microenvironment (TME), tumor tissue penetration, and cellular internalization. These factors collectively and significantly influence the manifestation and effectiveness of the EPR effect.[6] In this regard, the nanogold-albumin-based carriers, with albumin acting in stealth fashion towards the MPS, provide a means of precisely controlling the interactions at the nano–bio interface, facilitating the delivery of encapsulated drugs, genes, or other large molecules, offering a method for tailored therapeutic interventions (Table 4). Moreover, the ability to fine-tune the size, geometry, charge, and surface modifications of nanogold-albumin conjugates makes them well-suited for EPR-based cancer nanomedicine.

Striking a balance between the MPS and RES systems and precise control over drug release is critical for enhancing EPR-based targeting to ensure optimal delivery of therapeutic agents with nanogold-albumin conjugates. With this objective, Chiu *et al.* recently developed homogeneous core–shell gold nanorod/serum albumin (GNP@SA) co-loaded with doxorubicin (DOX) using glutaraldehyde (GTA) crosslinking (GNP@DOX:SAs (GTA)) or a denaturing method using methanol/ethanol (EM) (GNP@DOX:SAs (EM)).[117] The GTA cross-linked GNP@DOX:SAs show high colloidal stability and considerably low protein corona formation. The system exhibits reduced macrophage phagocytosis and increased interaction with cancer cells, resulting in higher cellular uptake. This GTA cross-linked nanogold-albumin could accommodate very high DOX loading of ~45% with <1% drug leakage in biological fluids and exhibits prolonged stability over a week in aqueous dispersions. Furthermore, GNP@DOX:SAs exert superior therapeutic efficacy and produced *in vivo* tumour growth inhibition upon NIR laser exposure as assessed by tail vein injections in prostrate tumour-bearing mice through combinatorial photothermal, photoacoustic, and chemotherapy approaches. Notably, the GNP@DOX:SAs (GTA) show greater accumulation at the tumour site than those produced with EM while reducing accumulation in RES clearance organs like the spleen, probably due to the EPR effect (Fig. 3A and B). The desolvation and glutaraldehyde cross-linking approach can be used for higher loading of the chemotherapeutic drug in albumin-stabilized gold nanorod conjugate (GNP@HSA-PTX).[118,119] Peralta *et al.* investigated the influence of cross-linking on the loading efficiency of the chemotherapeutic drug paclitaxel (PTX) in a nanogold-albumin conjugate developed using gold nanorods and HAS (GNP@HSA-PTX). Their findings revealed that the presence of nanorods resulted in a significant enhancement of drug-loading capacity, with an approximately 45% increase compared with albumin-only nanoparticles. Specifically, the nanogold-albumin carrier achieved a PTX loading of 91.8 ± 9 μg, compared with 63.3 ± 14 μg for the albumin-only system.[120] Furthermore, cross-linking with 20% and 40% of glutaraldehyde shows a variation in PTX loading capacity of 53 ± 49 μg and 92 ± 14 μg, respectively. GNP@HSA-PTX shows simultaneous chemotherapeutic and photothermal therapy on 4T1 breast cancer cells, with the bulk

Table 4 Nanogold-albumin conjugates for delivery of drugs and biologics in cancer therapy

Nanogold-albumin platform	Drug molecule	Type of modification/mechanism of drug loading	Tumor model	Ref.
Gold nanorods stabilized with serum albumin	Doxorubicin (DOX)	Glutaraldehyde cross-linking/alcohol denaturation of albumin DOX loading by electrostatic interaction	Tramp-C1, and RAW 264.7 cells	117
Gold nanorods encapsulated in HSA nanoparticles	Paclitaxel (PTX)	Glutaraldehyde cross-linking of albumin PTX loading by hydrophobic interaction	4T1 cells	120
Gold nanospheres stabilized with BSA	Gemcitabine	BSA acts as a reducing and stabilizing agent for GEM loading by electrostatic layer-by-layer assembly	A549 cells	122
Gold nanoclusters stabilized with BSA	GNC-BSA concentration-dependent cytotoxicity	BSA acts as a reducing and stabilizing agent	HepG-2 cells; nude BALB/c mice injected subcutaneously with HepG-2 cells	123
Gold nanoclusters stabilized with BSA	Curcumin	BSA and Cur act as reducing and stabilizing agents	HeLa and COS-7 cells	53
Gold nanoclusters stabilized with BSA in oil–water based nanocapsules	Curcumin	Self-assembled core–shell structure at oil–water interface stabilized by GNC-BSA and encapsulated with Cur in oil phase	SH-SY5Y cells	124
Gold nanoclusters stabilized with BSA	Kaempferol	BSA and kaempferol as reducing and stabilizing agents	A549 cells	125
Gold nanoclusters stabilized with BSA	DOX and SN-38 (camptothecin analogue)	Conjugation to BSA by disulphide and melamide linkers which are pH and redox sensitive	MCF-7, MDA-MB-231, and Panc-1 cells	126
Gold nanoclusters stabilized with BSA	Quercetin	Quercetin bound to GNC-BSA through Au-OH interactions	A549 cells	127
Gold nanoclusters stabilized with BSA	Paclitaxel and curcumin	PTX and Cur binds GNC-BSA through a hydrophobic interactions	KYSE150 cells	128

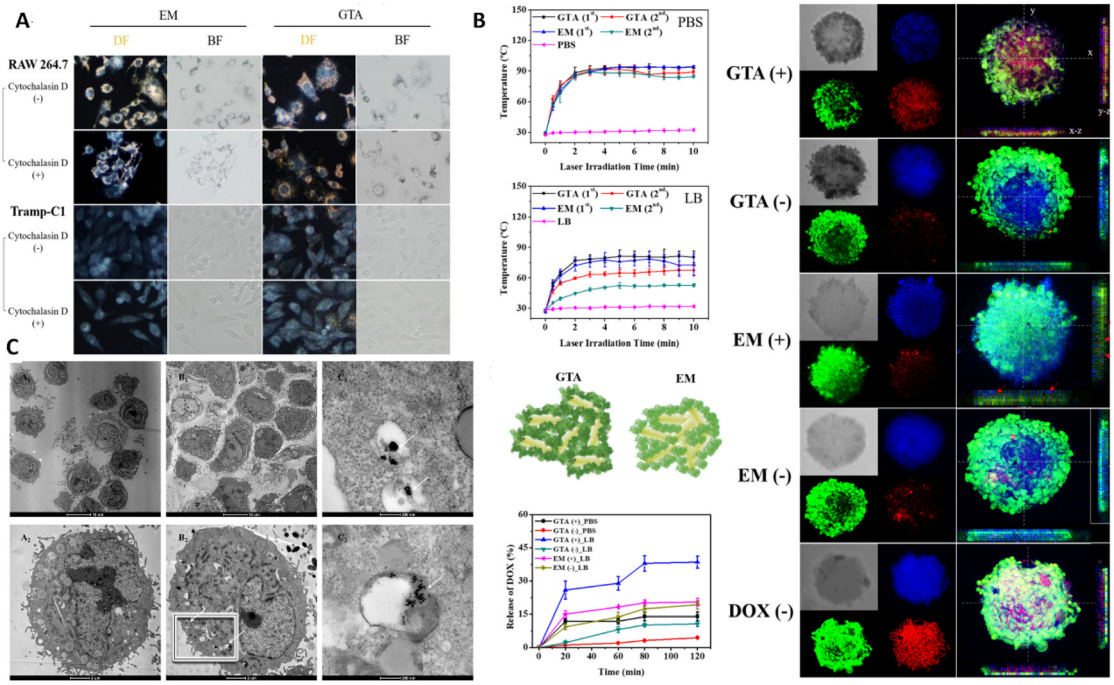

Fig. 3 Nanogold-albumin in passive targeting. (A) Dark-field images for uptake of GNP@SAs (GTA) and NR@SAs (EM) by RAW 264.7 macrophages and Tramp-C1 cancer cells with and without cytochalasin D pre-treatment; (B) evaluation of *in vitro* DOX penetration by GNP@DOX:SAs (GTA), GNP@DOX:SAs (EM), or free DOX in 3D tumor spheroids as observed using confocal microscopy; This figure has been adapted/reproduced from Chiu *et al.* with permission from the American Chemical Society, Copyright © 2018;[117] (C) TEM images of A549 cells with and without GNP@BSA-Gem treatment at different magnifications. This figure has been adapted/reproduced from Wang *et al.* with permission from Elsevier, Copyright © 2018.[122]

particle solution reaching temperatures of up to 46 °C following 15 minutes of NIR laser exposure. Treatment of 4T1 mouse breast cancer cells with GNP@HSA-PTX nanoparticles at a concentration of 20 μg PTX per mL causes approximately 82% cell death without irradiation and nearly 94% achieved after a single irradiation session. This hybrid nanogold-albumin system offers significant potential for integration with targeting ligands such as antibodies, enabling the development of a versatile and multimodal treatment platform for effective cancer management.

It is well established that positively charged nanoparticles exhibit improved cellular uptake due to ionic interactions with the negatively charged cell membrane.[121] In this regard, positively charged nanogold-albumin conjugates are promising platforms for loading negatively charged drug molecules through electrostatic interaction. Wang *et al.* developed BSA-stabilized gold nanospheres (GNP@BSA) with an approximate diameter of 10 nm through a facile one-pot synthesis method, utilizing the reduction of chloroauric acid ($HAuCl_4$) with BSA as the stabilizer and hydrazine monohydrate as the reducing agent. These nanoparticles exhibited a positive surface charge of 28.73 ± 0.92 mV. Gemcitabine, a chemotherapeutic agent with a net negative charge of −10.42 ± 1.44 mV, was then attached to the GNP@BSA through electrostatic layer-by-layer assembly, resulting in a final nanoconjugate (GNP@BSA-gemcitabine) with a positive surface charge of 5.07 ± 2.93 mV. *In vitro* assays in pulmonary carcinoma cells showed that the GNP@BSA system demonstrated high biocompatibility, while GNP@BSA-gemcitabine exhibited very high cell death compared with pristine gemcitabine (Fig. 3C).[122]

Nanogold-albumin derived from GNCs is extensively investigated as a drug delivery system, primarily without light activation. A pioneering study by Dong *et al.* reveals that BSA-stabilized GNCs could elicit a dose- and time-dependent decline in cell viabilities, and HUVECs (umbilical vein endothelial cells), which had a higher intake of GNC-BSA than A875 (melanoma cells), exhibited more toxicity. Furthermore, their research highlighted the significant inhibition of tumour growth in mouse models with subcutaneous HepG-2 liver tumours by GNC-BSA alone, suggesting its potential as a standalone anti-cancer agent. Interestingly, their findings indicated that GNC-BSA concentrations of 5 and 20 nM demonstrated substantial toxicity on tumour cells, impeding tumor growth and safeguarding the liver from tumour-induced effects.[123]

The nanogold-albumin conjugate can effectively deliver flavonoid-based drugs such as curcumin,[53,124] kaempferol,[125] and quercetin[127] for cancer therapy. Curcumin can directly be conjugated to BSA-capped GNCs (GNC-BSA-curcumin), which exhibit bright fluorescence ($\lambda_{ex}/\lambda_{em}$ = 550/650 nm) and show minimal toxicity in the normal kidney fibroblast cell line COS-7 (~100% cell survival) while displaying considerable

cytotoxicity and morphological damage in human cervical cancer cells HeLa (~15% cell survival) at a concentration of 100 μg mL^{-1}.[53] Curcumin can also be loaded in GNC-BSA nanocapsules by dissolving curcumin in the oil phase (composed of undecylenic acid) and mixing with the water phase consisting of GNC-BSA.[124] These nanocapsules demonstrate more significant growth inhibition of SH-SY5Y (neuroblastoma tumor cells, IC_{50} = 14.3 ± 0.35 nM) growth compared with free curcumin (IC_{50} = 115.6 ± 2.28 nM) or GNC-BSA (IC_{50} = 63.85 ± 2.79 nM) alone, probably due to a synergistic induction of cellular apoptosis for this particular nanocarrier system.[124] The natural flavonoid drug kaempferol can also be delivered by GNC-BSA conjugate (GNC-BSA-kaempferol), where the drug is stabilized *via* physical interactions with the nanogold-albumin.[125] The GNC-BSA-kaempferol conjugate demonstrates minimal to no toxicity toward HK-2 (normal human kidney cells), yet it successfully killed over 70% of A549 (lung cancer) cells at a concentration of 25 μg mL^{-1}. Furthermore, the GNC-BSA-kaempferol effectively reduced the migration rate of HeLa cells. Similarly, Lakshmi *et al.* developed a GNC-BSA platform to deliver the flavonoid quercetin.[127] Quercetin was bound to GNC-BSA through Au–OH interactions, and exhibits stable fluorescence ($\lambda_{ex}/\lambda_{em}$ = 360/568 nm) over a period of one month. This nanogold-albumin conjugate demonstrates efficient cellular uptake, and shows significant cytotoxicity against A549 (lung cancer) cells, with minimal toxicity towards HDFa (healthy fibroblast) cells.

Intracellular activation and controlled drug release are preferred strategies for effective chemotherapy in oncology. In this context, glutathione (GSH) offers a non-enzymatic mechanism for drug release. This approach leverages the significant disparity between intracellular GSH concentrations (1–10 mM) and extracellular thiol levels (2 μM glutathione and 8 μM cysteine).[129] Latorre *et al.* explored the potential of GNC-BSA as a nanocarrier for combined chemotherapy, primarily targeting cancer stem cells.[126] They functionalized the GNC-BSA with DOX and SN-38 (camptothecin analogue) to inhibit topoisomerase II and I in target cells. While clinical trials involving the combination of free DOX and SN-38 have shown limited success, previous studies indicated that this combination exhibits strong synergy when injected as a polymer–drug conjugate.[130] Thiol groups are introduced to the BSA with 2-iminothiolane. SN-38 is conjugated to the BSA using a redox-sensitive linker cleavable in reducing environments, such as those with high GSH or cysteine concentrations. Meanwhile, DOX was linked with a pH-sensitive linker susceptible to acidic environments, like those in endosomes and lysosomes. *In vitro* toxicity studies in MCF7, MDA-MB-231, and Panc-1 cell lines revealed that GNC-BSA loaded with DOX and SN-38 drugs displayed greater cytotoxicity than those loaded with only one of the drugs. These nanogold-albumin conjugates show good cellular uptake and bioimaging properties. Furthermore, therapy was achieved by significant DNA damage and antineoplastic activity against mammospheres even at very low concentrations of 0.08 μM, leading to an efficient reduction of the number of oncospheres and their size.[126]

3.2 Targeted delivery of therapeutic molecules

Successful delivery of therapeutics to disease sites poses a significant challenge in biomedicine. Two primary strategies for targeted therapeutics are: 'passive' targeting which relies on the EPR effect and active targeting which is achieved through tumor-avid functional moities. Despite the advantages, the significant limitation associated with passive targeting is suboptimal bio-distribution because of being trapped in the liver, spleen, or lung due to RES function. Additionally, heterogeneity and differences in vascular permeability lead to varied extents of the EPR effect even within the same tumour.[6] Furthermore, passive targeting is ineffective where tissue accumulation is not contingent upon EPR, such as vascular targeting, or when delivering therapeutic agents, which requires active transcytosis across physiological barriers like the intestinal mucosa or the blood–brain barrier. This holds specific importance for biomacromolecule payloads involving the RNAi pathway (including siRNA and miRNA), wherein cytosolic delivery is essential for bioactivity (Table 5).[131] In such situations, active targeting, achieved by conjugation of ligands or functional moieties including small molecules such as folic acid (FA), peptides, antibodies, or aptamers, that target overexpressed cell receptors or metabolic pathways, plays a vital role in directing nanoparticles specifically to malignant tissues. This targeted approach is especially beneficial in cancer therapy as it enhances the accumulation of the therapeutic agent in malignant tissues while minimizing off-target effects, thus increasing the efficacy and selectivity of the treatment.

The nanogold-albumin platform presents adaptable surface chemistry stemming from the GNP/GNC core and the albumin coating, including hydrophobic and hydrophilic regions and a high density of charged amino acids. This composition offers various chemically active groups for surface modification, allowing attachment of targeting agents and facilitating drug loading for cancer treatment applications.[19] Furthermore, the inherent ability of albumin to specifically bind to glycoprotein 60 (gp60) receptors and secreted protein acidic and rich in cysteine (SPARC) receptors on the cell surface endows nanogold-albumin conjugates with intrinsic targeting capabilities.[132] The gp60 receptor, found on vascular endothelial cells, facilitates the transport of albumin across the endothelial cell layer, while SPARC is highly expressed in various tumor cells and minimally present in normal tissues.[132] Spectroscopic studies of cisplatin-loaded albumin–GNP by Jaiswal *et al.* show that it could interact with glycans of the gp60 receptor and could effectively be used for *in vivo* or *in vitro* targeted drug delivery applications to cure cancer.[90] The interaction of nanogold-albumin with gp60 or SPARC receptors mainly depends on the structural integrity of surface albumin. Zhou *et al.* present a GNC-BSA-based theranostic nanoplatform designed for folate receptor (FR) targeted fluorescence imaging and chemotherapy of metastatic breast cancer. The GNC-BSA nanoparticles are covalently functionalized with modified PEG–folic acid (FA-PEG5k-COOH) as a targeting ligand and the hydro-

Table 5 Nanogold-albumin conjugates for targeted delivery of therapeutic molecules and biologics for cancer therapy

Nanogold-albumin platform	Therapeutic molecule	Targeting moiety/targeted receptor	Tumor model/cell lines	Ref.
Gold nanorods supramolecularly coated with biomimetic folic acid-modified BSA	EGFP and RNase A proteins	Folic acid (FA) for targeting folate receptor (FR)	HT29, and A549 cells	54
Gold nanoclusters stabilized with BSA and conjugated with methionine (Met)	Indocyanine green derivative (MPA) and DOX	Methionine (Met) metabolism targeting through LAT1 and LAT2 amino acid transporters	L02, Bel 7402, A549 and MCF-7 cells; MDA-MB-231, A549 and S180 tumor-bearing mice	55
Gold nanoclusters stabilized with BSA and conjugated with 6-thioguanine (6-TG)	Thioguanine (6-TG)	Albumin metabolism targeting in KRAS mutant cancer cells	HCT116 and A549 cells	56
Gold nanoclusters stabilized with BSA and modified with PEG-folic acid (FA-PEG5k-COOH)	Hydrophilic cisplatin prodrug (MDDP)	Folic acid (FA) for targeting folate receptor (FR-α)	4T1 cells; 4T1 tumor-bearing nude mouse model	133
Gold nanorods encapsulated in BSA shells	Bcl-2 specific SiRNA	Functionalization with anti-ErbB-2 *via* avidin-biotin chemistry for targeting ErbB-2 receptor	SK-BR-3, MCF-7, and HMEC cells	135
Gold nanospheres modified with BSA/HSA, anti-EGFR D-11 antibody and a Co(II) coordination compound $[CoCl(H_2O)(phendione)_2][BF_4]$ (TS265)	Co(II) coordination compound $[CoCl(H_2O)(phendione)_2][BF_4]$ (TS265) with proven anti-proliferative activity towards cancer cells	Anti-EGFR D-11 antibody	A549 and HCT116 cells; severe combined immunodeficient (NOD/SCID) male mice with HCT116-derived xenografts	137

philic cisplatin prodrug (MDDP). Upon intracellular activation of the cisplatin prodrug, the nanoparticles effectively induce significant cellular apoptosis. *In vivo* distribution analysis reveals that the nanoparticles efficiently evade reticuloendothelial system (RES) capture and preferentially accumulate in orthotopically implanted breast tumors. Additionally, the nanoparticles demonstrate high efficacy in simultaneously suppressing tumor growth and preventing lung metastasis in the 4T1 breast cancer model.[133]

One of the earliest hallmarks of cancer progression is the increased demand for amino acids or albumin, which can be exploited for active targeting of dysregulated metabolic pathways in cancer.[55] Chen *et al.* developed a GNC-BSA-based nanocomplex conjugated with methionine (Met) and indocyanine green (ICG) derivative (MPA) or DOX (GNC-BSA-Met-MPA and GNC-BSA-Met-DOX respectively) to target the L-type amino acid transporters LAT1 and LAT2, overexpressed in cancers, and responsible for trafficking methionine across the cell membrane.[55] The *in vitro* and *in vivo* studies showed excellent methionine metabolism targeting capability (Fig. 4A). Cellular studies in normal and cancer cells show a higher accumulation of GNC-BSA-Met-MPA in MCF-7 and GNC-BSA-Met-DOX in Bel-7402 (liver cancer) cells, respectively, which is consistent with the highly expressed LAT1 and LAT2 receptors on the two cell lines.[55,134] Furthermore, the *in vivo* studies also confirmed higher tumor-targeting and a greater distribution of GNC-BSA-Met-MPA in LAT1- and LAT2-positive tumor-bearing mouse models (MDA-MB-231) when compared with those of relatively low LAT1- and LAT2-expressing tumor models (A549).

Mutations in the Kirsten Rat Sarcoma Viral Oncogene Homolog (KRAS) exhibit increased macropinocytosis, enabling albumin uptake and making nanogold-albumin a promising tool to target aberrant nutrient metabolism in cancers.[136] Jaiswal *et al.* recently reported a fluorescent GNC-BSA conjugate for enhanced loading of the hydrophobic purine analogue drug 6-thioguanine (GNC-BSA-TG).[56] The release of 6-TG from the nanoconjugate, driven by cellular thiols such as glutathione (GSH), demonstrates its stimulus-responsive properties. Additionally, the nanoconjugate exhibits peroxidase-like enzyme activity, depleting cellular GSH levels and inducing oxidative stress, synergistically enhancing the chemotherapeutic efficacy of 6-thioguanine. Cytotoxicity analysis revealed a roughly 50% reduction in IC_{50} values for GNC-BSA-TG compared with free 6-TG in HCT116 and A549 cells with KRAS mutations, while KRAS wild-type HEK293T cells showed minimal toxicity under similar conditions. The enhanced albumin macropinocytosis in KRAS mutant cells likely facilitates a greater uptake of GNC-BSA-TG, leading to higher cancer cell death while sparing normal cells. The fluorescent nature of the 6-thioguanine-loaded GNC-BSA conjugate allows its uptake to be easily traced *via* fluorescence imaging (Fig. 4B). These findings underscore the potential of nanogold-albumin conjugates as targeted drug delivery carriers that exploit altered cancer metabolism.

Conjugation of targeting peptides/proteins or antibodies presents another paradigm for delivering cargo into cells. Research on peptide- or protein-coated GNPs predominantly explores the use of targeting peptide sequences or receptor-specific antibodies. Importantly, these surface modifications improve the particles' ability to enter various organelles or selectively target cancer cells. Achilli *et al.* demonstrated that GNPs can be coated with a cross-linked multilayer of albumin to produce a highly compact protein shell, preserving the structure of the most external layer of the nanogold-albumin.[138] Surface functionalization of these nanoconjugates with bombesin-related peptide shows enhanced *in vitro* uptake by PC-3 cells and a significant reduction of the corona effect.

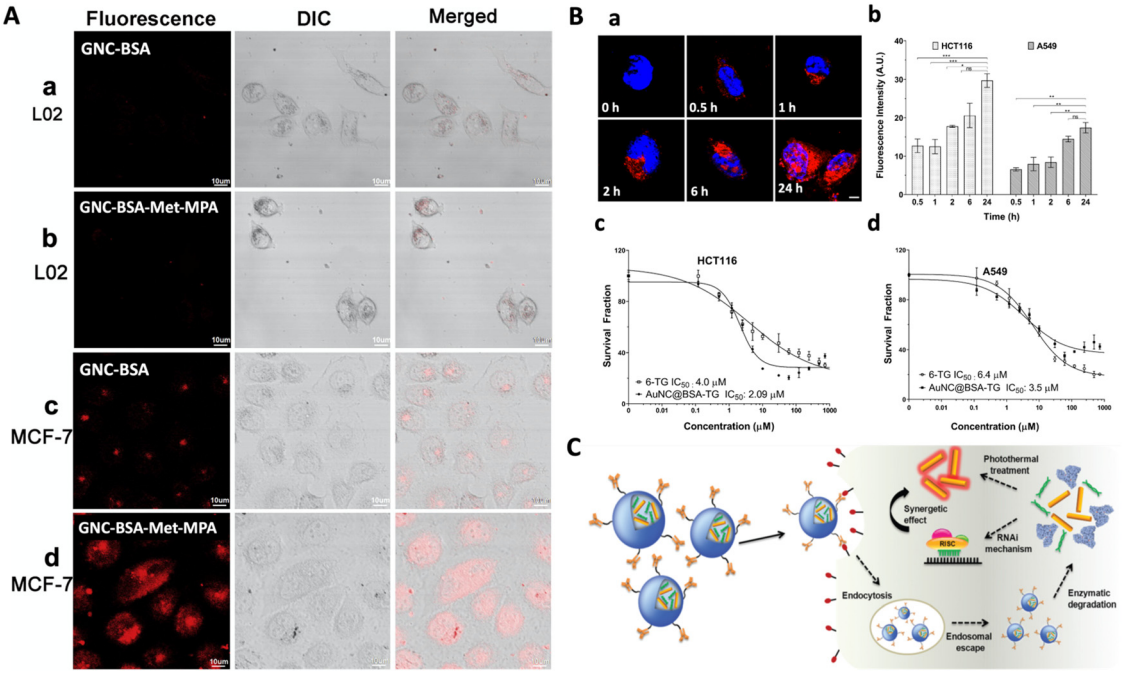

Fig. 4 Nanogold-albumin in active targeting. (A) The fluorescence microscopy images of GNC-BSA- and GNC-BSA-Met-MPA-treated L02 normal human cells (a and b) and MCF-7 (c and d) tumor cells. This figure has been adapted/reproduced from Chen *et al.* with permission from Elsevier, Copyright © 2012;[55] (B) intracellular uptake and therapeutic potential of GNC-BSA-TG in KRAS mutant HCT116 and A549 cells: (a) representative fluorescence microscopy images of HCT116 cells treated with GNC-BSA-TG over varying time intervals; (b) quantitative analysis of red fluorescence intensity showing time-dependent cellular uptake of GNC-BSA-TG in HCT116 and A549 cells; (c and d) cell viability of HCT116 and A549 cells following treatment with GNC-BSA-TG and free 6-TG. This figure has been adapted/reproduced from Jaiswal *et al.* with permission from Elsevier, Copyright © 2024;[56] (C) selective internalization of anti-ErbB-2 antibodies modified SREB nanocomplexes through active targeting to specific cancer cells by receptor-mediated endocytosis. This figure has been adapted/reproduced from Choi *et al.* with permission from RSC, Copyright © 2015.[135]

Tkachenko *et al.* developed an elegant nanogold-albumin conjugate by modifying gold nanospheres with BSA (GNP-BSA), which is pre-linked to different cellular targeting peptides.[139,140] The presence of albumin contributes significantly to the stability of GNP-BSA-peptide conjugates in serum-containing media. This GNP-BSA enters the nucleus of HepG2 cells when functionalized with targeting peptides containing sequences for receptor-mediated endocytosis (RME) and nuclear localization signals (NLS). Studies show that conjugating these sequences separately, rather than combining them into a single sequence, enhances nuclear targeting efficiency. The intracellular distribution of NLS sequences is further explored using GNP-BSA nanoconjugates modified with various NLS peptides in HeLa, 3T3, and HepG2 cells. Findings reveal that the transport of nanoparticles into the cytoplasm and nucleus depends on the peptide sequence and the cell type.[139] For instance, GNP-BSA modified with protein transduction domains (PTDs) from the HIV Tat protein are internalized into the cytoplasm but do not reach the nucleus in 3T3 and HepG2 cells. The uptake of these nanoparticles is temperature-dependent, suggesting the involvement of an endosomal pathway. In contrast, GNP-BSA functionalized with adenovirus-derived NLS and integrin-binding domains are internalized *via* an energy-dependent mechanism and successfully localized to the nucleus.[140] These observations suggest that combining specific targeting peptides on a single nanogold-albumin carrier offers the most efficient strategy for nuclear targeting. Furthermore, as BSA does not add greatly to the size of the GNPs, it may conveniently be used in constructing intracellular organelle targeting vectors, as only particles with diameters below 30 nm can enter cell nuclei. A significant study by Choi *et al.* reports the efficient ErbB-2 receptor-targeted delivery of Bcl-2 specific siRNA using a nanogold-albumin conjugate.[135] They developed a gold nanorod-BSA-based complex containing Bcl-2 specific siRNA and modified it with anti-ErbB-2 antibodies (SREB nanocomplexes). The SREB nanocomplexes show a high loading of 2×10^5 siRNA molecules and eight nanorods per BSA complex. The anti-ErbB-2 antibodies on the surfaces of SREB nanocomplexes enabled active targeting *via* selective receptor-mediated endocytic uptake by ErbB-2 receptor-overexpressing SK-BR-3 cells. The intracellular decomposition of the nanocomplexes by proteolytic enzymes led to an efficient synergistic anticancer effect, combining RNA interference-mediated silencing of Bcl-2 with the photothermal effect mediated by GNPs (Fig. 4C). These SREB nanocomplexes demonstrated potent *in vitro* efficacy, resulting in up to approximately 80% cancer cell death, with therapeutic effects sustained for around 72 hours, highlighting the possibility of

SREB nanocomplexes as a robust and effective theranostic tool *in vivo*. Fernandes *et al.* developed a multifunctional nanogold-albumin conjugate – TargetNanoTS265 – for targeted cancer therapy.[137] This system incorporates a monoclonal antibody against the epidermal growth factor receptor (EGFR) (anti-EGFR D-11) for active targeting and an anticancer cobalt(II) coordination compound, $[CoCl(H_2O)(phendione)_2][BF_4]$ (phendione = 1,10-phenanthroline-5,6-dione) (TS265). The formulation known as TargetNanoTS265 consists of ~14 nm GNPs functionalized with bifunctional polyethylene glycol (PEG) (SH-EG (8) $-(CH_2)_2$-COOH) to enhance stability and stealth properties *in vivo*, BSA/HSA to facilitate TS265 loading, and anti-EGFR D-11 antibody to target cancer cells exhibiting high EGFR expression. The efficacy of TargetNanoTS265 and its non-targeted counterpart (NanoTS265) tested *in vitro* on cancer cell lines and *in vivo* using mouse xenograft models demonstrates efficient and selective delivery of the cytotoxic payload, significantly enhancing tumor cell death compared with the free compound. In particular, treatment of HCT116-derived xenograft tumors with TargetNanoTS265 achieved a remarkable 93% tumor reduction. This formulation highlights the potential of nanogold-albumin-based systems for nanovectorizing chemotherapeutic agents. Its adaptable design, employing BSA or HSA conjugates for drug delivery, offers a versatile platform for controlled and selective targeting of diverse therapeutic agents to cancer cells.

3.3 Delivery of therapeutic proteins

The intracellular delivery of therapeutic proteins into cells presents a promising strategy for addressing "undruggable" diseases related to protein deficiencies and cancer.[141] Protein therapeutics are more effective at modulating cellular functions and treating various diseases, due to their high functional specificity and minimal side effects, than genetic therapies or small molecules.[3] However, the delivery of such protein biologics to the target sites has been the bottleneck of current approaches due to the high clearance, low plasma stability, and limited cellular uptake due to their relatively large sizes, hydrophilicity, and rapid degradation in the endo-/lysosomal compartments of cells.[142] The stability of the protein cargo against enzymatic digestion poses another major challenge.

Potentially, non-covalent conjugation of proteins of interest to the nanogold-albumin platform can address these limitations by preserving the structure and activity of the protein cargo. The nanogold-albumin conjugates provide a versatile platform for protein delivery, leveraging albumin's inherent capacity to form non-covalent interactions such as hydrogen bonding, van der Waals forces, and hydrophobic interactions. These properties of albumin ensure efficient loading and stabilization of proteins, making nanogold-albumin conjugates a promising tool for therapeutic applications. Khandelia *et al.* developed an innovative, self-assembled-GNP-lysozyme-albumin-based nanocarrier that can efficiently encapsulate both doxorubicin (DOX) and pyrene (Pyr) as model hydrophilic and hydrophobic drug molecules, respectively, with high loading capacity.[143] Negatively charged citrate-capped GNPs and positively charged lysozyme spontaneously assembled through complementary electrostatic interactions, followed by an albumin coating to enhance stability and biocompatibility. *In vitro* experiments show that the nanocarriers are successfully internalized by cancer cells, where they simultaneously release their payloads, resulting in cell death that is more effective than using the drug molecules alone. This innovative design exhibits no detectable cytotoxicity, underscoring its potential as a safe platform for protein-based therapeutic delivery. The incorporation of albumin leads to preferential intratumor accumulation of the nanocarrier.[143]

Modified nanogold-albumin-based carriers for the intracellular delivery of enhanced green fluorescent protein (GNP-BSA_{FA}-EGFP) and enzyme (GNP-BSA_{FA}-RNase A) have been synthesized by metal-directed assembly of EGFP and RNase A with a biomimetic folic acid-modified BSA corona, which can specifically target FR-overexpressing cancers for the delivery of therapeutics.[54] These nanogold-albumin-based EGFP and RNase A delivery nanocarriers exhibited high protein loading capacities of ~42 and ~54%, respectively, and high colloidal stability increased colloidal stability and rapid protein release in the presence of biological thiols. Furthermore, folate receptor-targeting facilitates receptor-mediated internalization and successful cytosolic delivery of EGFP and RNase A in HT29 cells (Fig. 5A and B). RNase A delivery in multicellular 3D spheroids of HT29 cells exhibits a radical reduction in the cellular RNA, signifying RNA degradation and resulting in subsequent cell death (Fig. 5B). The study represents the first proof of concept on folic acid-modified nanogold-albumin as a targeting and antifouling platform for enhanced intracellular EGFP and RNase A delivery. Such nanoconjugates could be adapted to efficiently deliver therapeutic proteins, a forward-looking perspective for the targeted delivery of therapeutic proteins and enzymes, with enormous potential as a safe and efficacious platform for application in protein-based cancer therapeutics.

In recent years, cancer immunotherapy has emerged as a promising approach for cancer therapy with fewer side effects by directly engaging the immune system, particularly in cases where traditional therapies are ineffective. They function by delivering antigenic information to dendritic cells (DCs), which subsequently stimulate an immune response. However, cancer immunotherapy faces significant challenges, including limited immune cell proliferation and the highly immunosuppressive nature of the tumor microenvironment, which hinder its overall effectiveness. Nanogold-albumin conjugates can be a valuable tool in addressing these challenges by enhancing the delivery and stability of antigens, facilitating the activation of dendritic cells, and modulating the tumor microenvironment to overcome immune suppression. A recent study by Zafar *et al.* study proposes a novel nanogold-albumin conjugate composed of HSA-copper complex-loaded gold nanocages coated with bacterial membranes (GNP-HSA-Cu) targeting the cuproptosis–lactate regulation pathway to induce cuproptosis and enhance anti-tumor immunity.[144] The near-infrared (NIR) active gold nanocages release the HSA-copper complex,

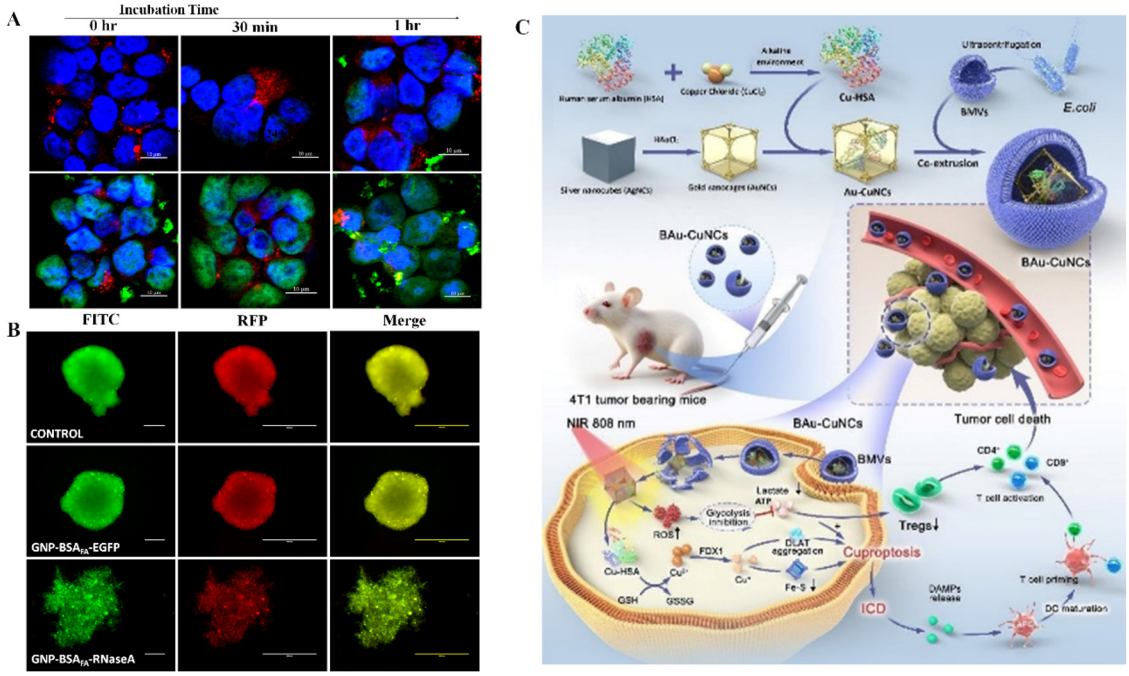

Fig. 5 Nanogold-albumin-based protein therapeutics. Time-dependent intracellular protein delivery by GNP-BSA$_{FA}$-EGFP in HT29 (FR+) cells. (A) Fluorescence microscopy images of HT29 cells treated with GNP-BSA$_{FA}$-EGFP for t = 0, 0.5, 1, 2, 4, and 24 h; (B) intracellular RNA degradation efficacy of GNP-BSA$_{FA}$-RNaseA in 3D spheroids of HT29 cells for untreated (control), GNP-BSA$_{FA}$-EGFP, and GNP-BSA$_{FA}$-RNaseA-treated HT29 spheroids stained with AO for differential staining of total cellular DNA and RNA. This figure has been adapted/reproduced from Jaiswal *et al.* with permission from Elsevier, Copyright © 2022;[54] (C) schematic illustration of HSA-copper complex-loaded gold nanocages coated with bacterial membranes (GNP-HSA-Cu) targeting the cuproptosis–lactate regulation pathway to induce cuproptosis and enhance anti-tumor immunity. This figure has been adapted/reproduced from Zafar *et al.* with permission from Elsevier, Copyright © 2024.[144]

enabling its reaction with intratumoral GSH through a disulfide exchange reaction, thereby releasing Cu^{2+} ions and inducing cuproptosis. Induction of cuproptosis subsequently initiates immunogenic cell death (ICD) by releasing damage-associated molecular patterns (DAMPs), which stimulate robust anti-tumor immunity by activating cytotoxic $CD8^+$ T cells and helper $CD4^+$ T cells. Concurrently, NIR irradiation of the gold nanocages generates excessive reactive oxygen species (ROS), significantly inhibiting glycolysis and reducing lactate and ATP levels. This cascade of reduced lactate production, ATP depletion, and GSH consumption sensitizes tumor cells to cuproptosis. Moreover, the lower lactate levels effectively suppress immunosuppressive T regulatory cells (Tregs), further enhancing anti-tumor immunity. This innovative nanogold-albumin conjugate effectively inhibits breast cancer metastasis to the lungs, amplifying the therapeutic impact of the GNP-HSA-Cu + NIR treatment. This study introduces a novel platform for cuproptosis–lactate regulation, offering a highly innovative and effective strategy to develop nanogold-albumin conjugates for tumor immunotherapy.

Among the various immunotherapy strategies, therapeutic cancer vaccines aim to activate the adaptive immune system to target and eliminate cancer cells. These vaccines represent a significant advancement in cancer treatment by enhancing the immune system's therapeutic potential. However, the efficacy of many cancer vaccines remains limited due to challenges such as insufficient stability, inadequate immune activation, and the lack of effective adjuvants. Recent research has demonstrated that photothermal therapy (PTT) holds significant promise as a potent adjuvant for immunotherapy, as it can stimulate the release of tumor-associated antigens, thereby recruiting the immune cells necessary to initiate a robust immune response. In this context, gold nanoparticles (GNPs) are exemplary photosensitizers for PTT, and albumin, which contains numerous disulfide bonds, is sensitive to elevated levels of glutathione (GSH) in tumor microenvironments, making nanogold-albumin a suitable carrier for tumor-targeted therapies. Zhang *et al.* recently reported a nanogold-albumin conjugate composed of self-generated GNPs templated by human serum albumin (HSA), encapsulating the hydrophilic human melanoma antigen $gp100_{25-33}$ (hgp100) peptide. This peptide is known for its ability to stimulate a specific immune response due to its high expression in melanoma, one of the most aggressive skin cancers.[145] The GNP-HSA conjugate effectively shields the peptide in physiological environments, enabling controlled drug release triggered by near-infrared (NIR) irradiation and elevated GSH levels at tumor sites. The PTT mediated by GNP-HSA ablates tumors and promotes the release of endogenous tumor antigens, which, together with hgp100, induce immune activation and dendritic cell maturation. *In vivo* results demonstrate that dendritic cell maturation and specific hgp100 cross-presen-

tation are significantly enhanced in the lymph nodes, spleen, and tumor microenvironment. This dual action of local PTT and immune amplification establishes GNP-HSA as a highly efficient cancer vaccine platform with potential applications across various diseases.

3.4 Bio-imaging

Bio-imaging plays a critical role in cancer diagnosis and treatment by providing precise, detailed visualization of tumors within the body. Advanced imaging techniques, including fluorescence imaging, magnetic resonance imaging (MRI), positron emission tomography (PET), and optical coherence tomography (OCT), offer high-resolution, real-time insights into tumor morphology, vascularization, and metabolic activity. Among these, fluorescence imaging is particularly notable for its non-invasive nature and exceptional spatial resolution, making it highly effective for early-stage tumor detection and accurate diagnosis. Additionally, it enables real-time monitoring of tumor progression and treatment response, thereby enhancing the precision and efficacy of cancer therapies. Notably, nanogold-albumin, particularly ultra-small GNC-BSA, exhibits intriguing fluorescence properties derived from the Au_{25} core, further expanding its potential in advanced bio-imaging applications (Table 6).[73] GNC-BSA demonstrates favorable physicochemical attributes and biocompatibility due to the presence of the serum albumin in GNC-BSA, enabling it to overcome inherent issues associated with conventional imaging agents, such as organic dyes, which are prone to photobleaching or phototoxicity, and QDs, which entails harsh synthetic conditions and high cytotoxicity, making them a promising class bio-imaging agents.[146,147]

Zhang *et al.* synthesized vibrant red fluorescence-emitting GNC-BSA with a quantum yield of ~9.4% and used it for rapid imaging of tumor cells.[146] The GNC-BSA did not display cell cytotoxicity in the 0.1–10 mg mL^{-1} concentration range towards MCF-7, HeLa, L02, U87, and A549 cells (Fig. 6A and B). Moreover, prepared GNC-BSA, when used as an *in vitro* and *in vivo* cancer imaging modality, showed excellent tumor-targeted imaging in a relatively short period (Fig. 6C–F). GNC-BSA may also be modified with specific molecules to impart cell receptor targeting functionality. Retnakumari *et al.* functionalized GNC-BSA with folic acid (FA) to target overexpressed folate receptors (FRs).[105] They observed a significantly high accumulation of the fluorescent GNC-BSA in FR-overexpressing KB (oral squamous cell carcinoma) compared with FR-negative MCF-7 (breast adenocarcinoma) cells. A similar observation was reported by Zhang *et al.* where GNC-BSA coated with FA or hyaluronic acid (HA) exhibited strong red fluorescence under a UV lamp (λ_{ex} = 365 nm) with a high fluorescence QY of 14.8 ± 2.2%. Modifying these nanogold-albumin conjugates with FA or HA (GNC-BSA-FA/HA) as a recognition component for active tumor-targeted imaging exhibits strong red fluorescence in the FR overexpressing HEp-2 (hepatocellular carcinoma) cells. In contrast, very weak fluorescence is seen for FR-negative A549

Table 6 Nanogold-albumin conjugates for bio-imaging in cancer diagnosis

Nanogold-albumin platform	Cell line/model used	Imaging mode(s)	Remarks	Ref.
GNC-BSA	MCF-7 and HeLa cells; athymic nude mice	Near-infrared fluorescence (NIRF)	Fast synthesis of GNC-BSA at 80 °C for 10 min compared with that at 37 °C for 12 h	146
GNC-BSA	MDA-MB-45 and HeLa cells	Fluorescence microscopy	High accumulation in the tumor areas due to the enhanced permeability and retention (EPR) effects	150
GNC-BSA	Mice	2D and 3D ++ tomography (CT)	Can be clear visualization of the renal collecting system and ureters	151
GNC-BSA-p	HeLa cells	Confocal fluorescence microscopy	A polymer-like shielding layer significantly improves the stability of AuNCs against ROS and protease degradation; carbodiimide-activated coupling	152
GNC-BSA-SiNPs	A549 cells	Confocal fluorescence microscopy	Improved photostable and chemical stable properties	153
GNC-BSA-Her	ErbB-2^+ breast tumor	Confocal fluorescence microscopy	Specific targeting and nuclear localization in ErbB2-over-expressing breast cancer cells, for simultaneous imaging and cancer therapy	154
GNC-BSA-DOX	HeLa cells	Two-photon excitation	NIR excitation and emission (650–900 nm), ideal potential platform for imaging-guided drug delivery	81
GNC-BSA-RGD	U87-MG cells	One-photon/two-photon fluorescence microscopy	Polymeric nano-capsules loaded with GNCs specifically target U87-MG cancer cells overexpressing integrin anb3	155
GNC-BSA-NHA	BxPC-3 and HT-1080 tumor-bearing mice	Computed tomography (CT)	Imaging of hypoxia in the tumor microenvironment	156
GNC-BSA-iodine	Thyroid tumor-bearing mice	Fluorescence microscopy/ CT	Produce sensitive and accurate diagnosis of minimal thyroid cancer, as small as 2 mm^3	157
GNC-BSA-Gd_2O_3	U87-MG tumor-bearing mice	Fluorescence/MRI	Modification with arginine–glycine–aspartic acid peptide c(RGDyK) (RGD) enabled the nanoprobe for targeted tumor imaging *in vivo*	158
GNC-BSA-Gd	MCF-7 tumor-bearing mice	NIRF/CT/MRI	Ultrasmall hybrid NCs penetrate into the solid tumor for cancer targeted imaging and diagnosis *in vivo*	159
GNC-BSA-Gds-FA	KB tumor-bearing mice	Optical/MRI/CT	Very clear structural and anatomical information can be obtained; show good biocompatibility, quick renal clearance, and do not induce normal tissue toxicity *in vivo*	160

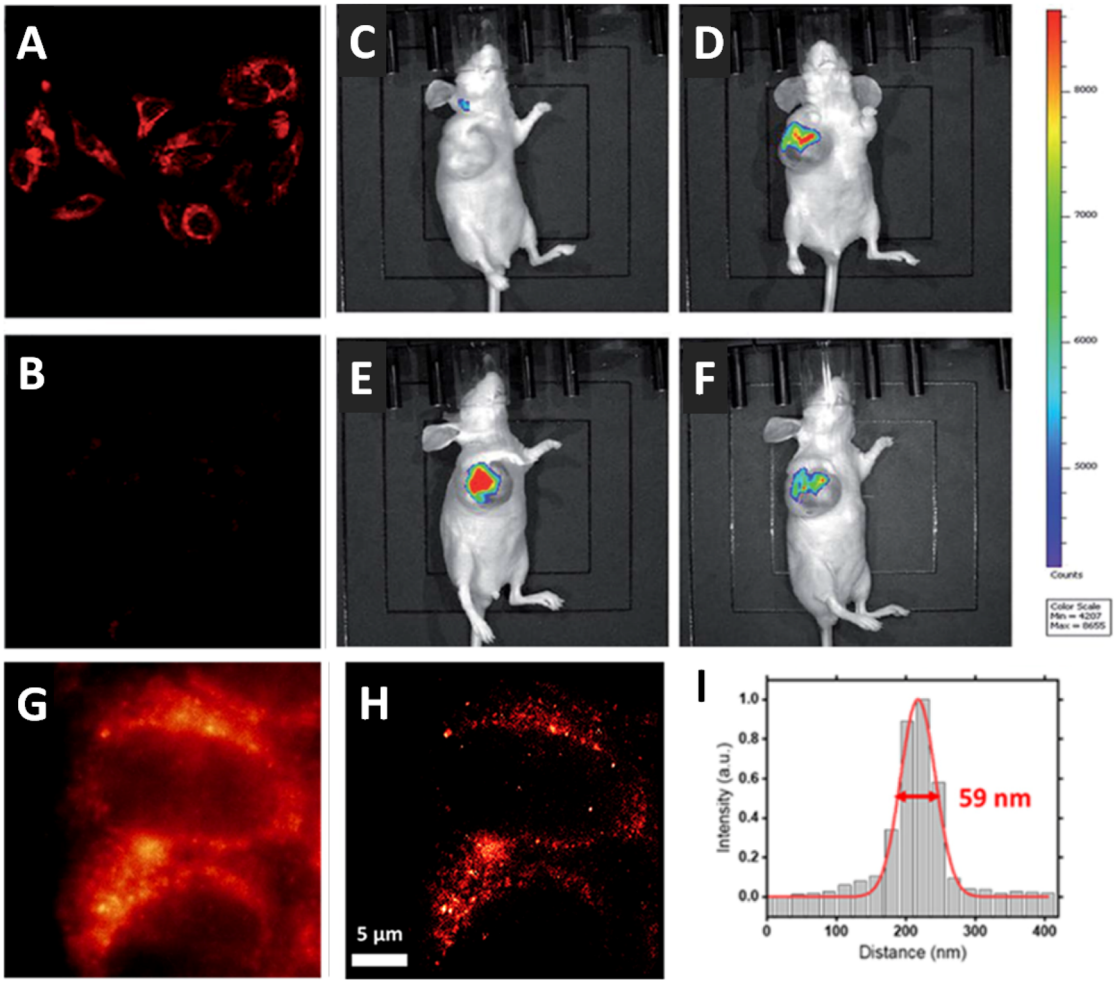

Fig. 6 Representative *in vitro* and *in vivo* bio-imaging applications of GNC-BSA bioconjugates. Laser confocal fluorescence micrographs of (A) HeLa cells and (B) L02 cells treated with 1 mg mL^{-1} GNC-BSA for 4 h; fluorescence imaging of xenograft tumour nude mice after intratumoral injection of 10 mg mL^{-1} GNC-BSA for varying times: (C) 0 min, (D) 30 min, (E) 60 min, and (F) 120 min. This figure has been adapted/reproduced from Zhang *et al.* with permission from RSC, Copyright © 2015;[146] (G) total internal reflection fluorescence (TIRF) image; (H) super-resolution radial fluctuation (SRRF) image of GNC-BSA-treated HeLa cells for labeling lysosomes and (I) The localization average pattern obtained from SRRF microscopy for lysosomes present. This figure has been adapted/reproduced from Yadav *et al.* with permission from Elsevier, Copyright © 2020.[149]

cells. HA functionalization results in the significant accumulation of GNC-BSA-HA in CD44-overexpressing A549 cells. Fluorescence studies *in vivo* in tumor-bearing nude mice show selective accumulation of the GNC-BSA-FA/HA in either HeLa or Hep-2 tumors, respectively.[148] These findings establish that GNC-BSA could be used for active targeting and sensitive imaging of cell-associated receptors for rapid tumor diagnosis in future clinical applications.

Nanogold-albumin conjugates (GNC-BSA/HSA) demonstrate significant potential as probes for advanced imaging techniques, including single-molecule super-resolution microscopy. These probes enable fluorescence visualization of complex cellular dynamics, such as those of the cytoskeleton, with nanometer-scale resolution *in vitro*.[161] Recently, Yadav *et al.* employed GNC-BSA as a highly effective nanoprobe for lysosomal imaging in HeLa cells.[149] The super-resolution radial fluctuation images revealed lysosomal structures with finer detail and reduced background noise compared with conventional fluorescence imaging (Fig. 6G and H). The average localization pattern of lysosomes is obtained with a maximum resolution of approximately 59 nm, closely resembling the original diameter of the smallest lysosome at around 50 nm in HeLa cells (Fig. 6I). These findings highlight the potential of nanogold-albumin conjugates as specific markers for super-resolution microscopy, offering a promising tool for high-precision imaging of various cellular organelles and advancing the field of cellular imaging and diagnostics.

3.5 Bio-sensing

The precise detection and quantification of disease-specific biomarkers are critical for early cancer diagnosis, enabling effective clinical intervention, timely treatment planning, and accurate prognosis assessment. In cancer, metastasis to distant tissues is a key driver of mortality, accounting for over

90% of cancer-related deaths.[162] It is a complex process in which tumor cells detach from the primary site, enter the bloodstream, and form secondary tumors in distant organs, significantly contributing to cancer-related morbidity and mortality.[163,164] The blood of cancer patients contains valuable biomarkers, including circulating tumor DNA (ctDNA), tumor-derived extracellular vesicles (tEVs), and circulating tumor cells (CTCs), which facilitate early detection and disease monitoring.[165–167] In this context, nanogold-albumin conjugates, due to their unique optical, electronic, and physicochemical properties, serve as potential platforms for developing ultrasensitive nanoassays.[167] Sensitive detection of cancer-related biomarkers is possible through a range of nanogold-albumin facilitated analytical approaches, including surface-enhanced Raman scattering (SERS),[168] fluorescence imaging,[166,169–171] electrochemical methods, *etc*., for enhancing diagnostic accuracy, prognostic evaluation, and overall survival outcomes for cancer patients.

Circulating tumor cells (CTCs) have garnered increasing attention in medical biology and clinical practice, particularly for their applications in cancer diagnosis, prognosis, and treatment monitoring. Detecting CTCs within the vast population of healthy blood cells remains a significant challenge due to their scarcity, necessitating the development of detection methods with exceptional sensitivity and specificity. CTCs initiate metastases and carry genetic information reflective of the primary tumor.[172] High levels of CTCs in the bloodstream are often associated with a poor prognosis, indicating their potential as biomarkers for tracking cancer progression and predicting patient outcomes.[162,163] Regular monitoring of CTC concentrations can aid in devising personalized treatment approaches by providing insights into real-time therapeutic responses. Wu *et al.* developed three kinds of surface-enhanced Raman scattering (SERS)-based nanogold-albumin conjugates consisting of gold nanospheres, nanorods, and nanostars conjugated with 4-MBA (4-mercaptobenzoic acid, a Raman reporter) and stabilized with FA-modified BSA.[168] These nanogold-albumin conjugates are employed to detect cancer cells in the peripheral blood of rabbits without the need for an enrichment process. Stabilization with reductive BSA minimizes nonspecific binding and uptake by healthy blood cells, ensuring excellent specificity. Additionally, conjugation with FA as a targeting ligand enhances sensitivity by facilitating the identification of CTCs. The specificity and sensitivity of the three SERS-active nanoparticles are assessed using HepG2 and HeLa cells, as HepG2 cells lack folate receptor alpha (FRα), while HeLa cells are FRα-positive. White blood cells (WBCs) served as a control due to their low FRα expression.[173] The study established that all three nanogold-albumin conjugates could be utilized for CTC detection in the blood with high specificity without the need for enrichment. The nanostar-based conjugate is the best due to its super-sensitivity with a limit of detection (LOD) of 1 cell per mL, whereas the LOD for both nanospheres and nanorods is 3 cells per mL. These findings highlight the potential of SERS-based nanogold-albumin conjugates as highly sensitive and specific tools for CTC detection, offering advancements in cancer diagnostics and monitoring.

The simultaneous enrichment and detection of circulating tumor cells (CTCs) provide invaluable insights for comprehensive cancer diagnosis, accurate prognosis, improved patient outcomes, and the development of personalized medicine.[174–176] Li *et al.* recently reported the development of an antifouling surface composed of silicon nanowires (SW) as a substrate, coated with amyloid-like transformed BSA inlaid with GNPs, and modified with sgc8 aptamer as a recognition group that can exclusively recognize overexpressed protein tyrosine kinase 7 (PTK7) in tumor cells.[166] The amyloid-transformed BSA coating embedded with gold nanoparticles provided a uniform antifouling surface, significantly reducing fouling by blood components, including human serum albumin (HSA), platelet-rich plasma (PRP), and white blood cells (WBC) by 88.5%, 88.0%, and 83.7%, respectively. The amyloid-transformed BSA, integrated with gold nanoparticles, also offered abundant sites for aptamer crosslinking, enhancing its functional versatility. The optimal conditions for target cell capture were assessed using MCF-7 cells (high PTK7 expression) and PC-3 cells (low PTK7 expression) on nanogold-albumin-modified SW surfaces over incubation times ranging from 10 to 40 minutes. At 30 minutes, fluorescence microscopic surface analysis shows an efficient capture rate of 85.2% for MCF-7 cells, with only 1.9% retention of PC-3 cells, demonstrating its ability to selectively isolate PTK7-expressing cells while minimizing nonspecific adhesion. Further studies with untreated blood samples show that the surfaces can capture approximately six cells per mL of fresh whole blood spiked with 10 cells. The nanogold-albumin surfaces additionally facilitated selective cell capture, with gentle and non-destructive release, and preserved the high viability of captured cells following incubation with GSH, attributed to their excellent biocompatibility.

GNC-BSA-stabilized fluorescent polystyrene (PS) nanoparticles modified with EpCAM aptamer (GNC-BSA-PS-Apt) have also been used to efficiently detect breast cancer cells based on a dual-fluorescence signal approach[169] (Fig. 7). The GNC-BSA adsorbed *via* electrostatic interaction imparted excellent colloidal stability and photostability to PS nanoparticles and abundant active linking sites for EpCAM aptamers. Quantitative analysis revealed approximately 198 EpCAM aptamers present per GNC-BSA-PS-Apt nanoparticle, which gave a strong green fluorescent signal from the GNC-BSA-PS-Apt that was observed on MCF-7 cells (Fig. 7A). In contrast, only a weak signal is detected on HEK-293T and MCF-10A cells, indicating that the interaction of GNC-BSA-PS-Apt with MCF-7 cells is primarily mediated by EpCAM aptamer targeting. The dual-fluorescence (green and red) signals from the fluorescent PS nanoparticles and GNC-BSA ensured high specificity for cell detection, minimizing the risk of false positives (Fig. 7B). The exceptional targeting capability of the nanogold-albumin platform was further demonstrated in xenograft tumor models of MCF-7 and HeLa cells in BALB/c nude mice, showing selective binding to EpCAM-positive MCF-7 breast tumor tissues with no interaction observed with EpCAM-negative HeLa tissues[169]

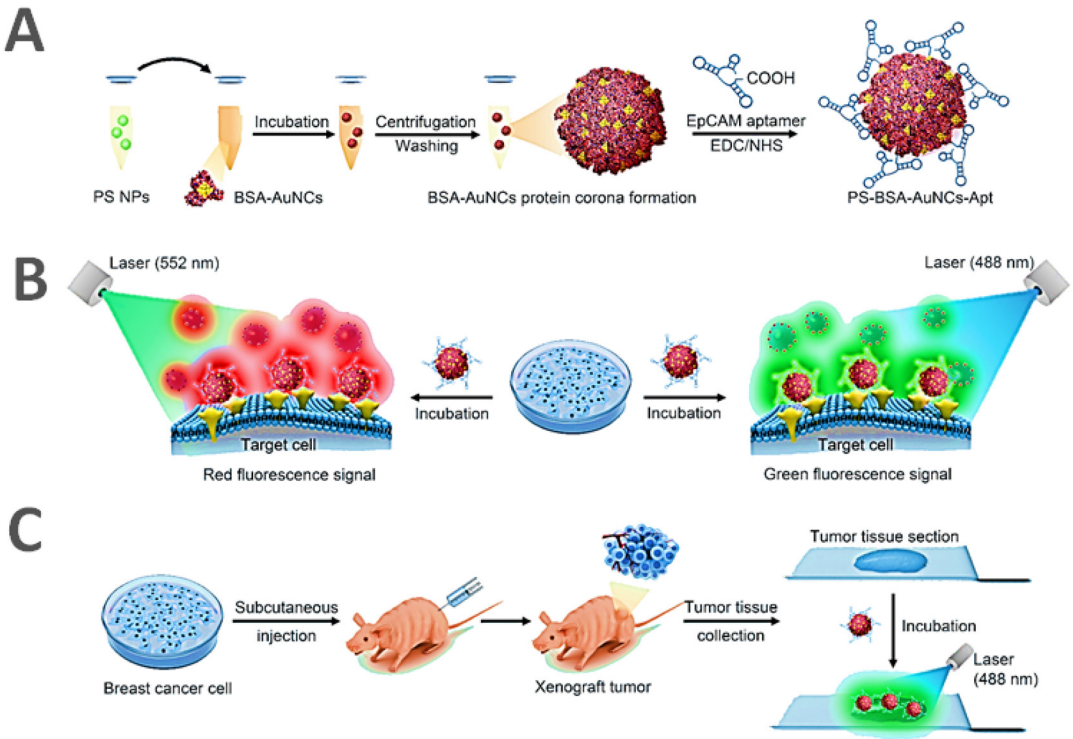

Fig. 7 Schematic illustration of the workflow for detecting EpCAM-positive breast cancer cells by GNC-BSA-PS-Apt. (A) Fabrication of GNC-BSA-PS-Apt. (B) Detection of breast cancer cells based on dual-color fluorescence signals. (C) Detection of xenografted breast tumor tissue. This figure has been adapted/reproduced from Wu *et al.* with permission from Elsevier, Copyright © 2022.[169]

(Fig. 7C). These studies provide a comprehensive insight into the innovative application of nanogold-albumin conjugates in developing liquid biopsy-based biosensors to enrich biomarkers from complex biological fluids efficiently. It extends beyond the traditional understanding of these conjugates as mere delivery vehicles, highlighting their potential as multifunctional platforms in biomedical diagnostics.

4 Summary and outlook

Nanogold-albumin conjugates are emerging as innovative tools in nanomedicine, offering significant potential for cancer therapy and diagnostics. These versatile systems are especially well-suited for theranostic applications, seamlessly integrating therapeutic, diagnostic, and bio-sensing functionalities. They are developed through two primary strategies: (1) supramolecular coating of GNPs with albumin *via* electrostatic or hydrophobic interactions(GNP-BSA/HSA) and (2) albumin-templated *in situ* synthesis of ultra-small gold nanoclusters (GNC-BSA/HSA). Both systems serve as flexible platforms for delivering diverse therapeutics, from small molecules to larger biomolecules, while offering promising applications in cancer monitoring and management. The synergy between gold and albumin endows these constructs with several key advantages, including low inherent toxicity, a high surface area, adjustable surface chemistry, distinctive optical properties and an extended shelf-life. These attributes enhance their suitability for clinical applications. Furthermore, albumin's natural affinity for receptors such as gp60 and SPARC—commonly overexpressed in tumor tissues—facilitates the selective accumulation of nanogold-albumin constructs in cancer cells, improving intratumoral drug delivery.

Despite their potential, several challenges hinder the clinical translation of nanogold-albumin conjugates. Although nanogold platforms such as AuroLase and CYT-6091 have entered clinical trials, widespread adoption remains limited due to issues related to reproducibility, batch consistency, long-term stability, and immune responses. Unlike conventional chemotherapy and antibody–drug conjugates, which benefit from well-established manufacturing pipelines, nanogold-albumin conjugates require precise control over surface characteristics such as charge, hydrophobicity, and functional group composition to optimize interactions with the tumor microenvironment. The incorporation of targeting ligands can further enhance the specificity; however, such modifications necessitate careful calibration to maintain the structural and functional integrity of the constructs. A comprehensive understanding of cellular uptake mechanisms and nanoparticle interactions within the tumor microenvironment is crucial to ensure the scalability and clinical viability of these platforms.

Beyond formulation challenges, the translation of nanogold-albumin conjugates from laboratory research to clinical

application is impeded by regulatory, economic, and scalability constraints. Maintaining precise control over nanoparticle size, shape, and albumin interactions at a commercial scale requires advanced and costly fabrication techniques. Additionally, regulatory approval for nanoparticle-based therapeutics is particularly stringent, requiring extensive preclinical and clinical validation to ensure long-term safety, biocompatibility, and efficacy.

Addressing these challenges through continued research, optimization of fabrication processes, and advancements in regulatory frameworks will be essential for the successful clinical translation of nanogold-albumin conjugates. The development of cost-effective and scalable synthesis techniques, coupled with a deeper understanding of nanoparticle interactions in biological systems, could facilitate their transition from experimental models to widely available therapeutic options. With further innovations, nanogold-albumin conjugates can potentially drive a paradigm shift in modern cancer nanomedicine, offering more effective, targeted, and less toxic alternatives to existing treatment modalities. Their multifunctional nature and ability to integrate therapy with real-time diagnostics underscore their potential to significantly enhance patient outcomes and redefine cancer management in the future.

Data availability

No primary research results, software or code have been included and no new data were generated or analysed as part of this review.

Conflicts of interest

There are no conflicts of interest to declare.

Acknowledgements

The authors express their gratitude to the Director of CSIR-CMERI, Durgapur, and the Director of NIT Durgapur for their support and encouragement. They also extend their thanks to the Department of Biotechnology, India, for financial support (BT/PR49579/MED/32/849/2023, GAP-245112).

References

1 H. Sung, J. Ferlay, R. L. Siegel, M. Laversanne, I. Soerjomataram, A. Jemal and F. Bray, Global Cancer Statistics 2020: GLOBOCAN Estimates of Incidence and Mortality Worldwide for 36 Cancers in 185 Countries, *CA-Cancer J. Clin.*, 2021, **71**, 209–249, DOI: **10.3322/caac.21660**.

2 K. Sathishkumar, M. Chaturvedi, P. Das, S. Stephen and P. Mathur, Cancer incidence estimates for 2022 & projection for 2025: Result from National Cancer Registry Programme, India, *Indian J. Med. Res.*, 2022, **156**, 598, DOI: **10.4103/ijmr.ijmr_1821_22**.

3 N. Serna, L. Sánchez-García, U. Unzueta, R. Díaz, E. Vázquez, R. Mangues and A. Villaverde, Protein-Based Therapeutic Killing for Cancer Therapies, *Trends Biotechnol.*, 2018, **36**, 318–335, DOI: **10.1016/j.tibtech.2017.11.007**.

4 R. K. Kankala, C.-G. Liu, A.-Z. Chen, S.-B. Wang, P.-Y. Xu, L. K. Mende, C.-L. Liu, C.-H. Lee and Y.-F. Hu, Overcoming Multidrug Resistance through the Synergistic Effects of Hierarchical pH-Sensitive, ROS-Generating Nanoreactors, *ACS Biomater. Sci. Eng.*, 2017, **3**, 2431–2442, DOI: **10.1021/acsbiomaterials.7b00569**.

5 P. Singh, S. Pandit, V. R. S. S. Mokkapati, A. Garg, V. Ravikumar and I. Mijakovic, Gold Nanoparticles in Diagnostics and Therapeutics for Human Cancer, *Int. J. Mol. Sci.*, 2018, **19**, 1979, DOI: **10.3390/ijms19071979**.

6 J. Shi, P. W. Kantoff, R. Wooster and O. C. Farokhzad, Cancer nanomedicine: progress, challenges and opportunities, *Nat. Rev. Cancer*, 2017, **17**, 20–37, DOI: **10.1038/nrc.2016.108**.

7 S. M. van de Looij, E. R. Hebels, M. Viola, M. Hembury, S. Oliveira and T. Vermonden, Gold Nanoclusters: Imaging, Therapy, and Theranostic Roles in Biomedical Applications, *Bioconjugate Chem.*, 2022, **33**, 4–23, DOI: **10.1021/acs.bioconjchem.1c00475**.

8 P. K. Gupta, Drug Targeting in Cancer Chemotherapy: A Clinical Perspective, *J. Pharm. Sci.*, 1990, **79**, 949–962, DOI: **10.1002/jps.2600791102**.

9 H. Y. Choi and J.-E. Chang, Targeted Therapy for Cancers: From Ongoing Clinical Trials to FDA-Approved Drugs, *Int. J. Mol. Sci.*, 2023, **24**, 13618, DOI: **10.3390/ijms241713618**.

10 A. O. Elzoghby, W. M. Samy and N. A. Elgindy, Albumin-based nanoparticles as potential controlled release drug delivery systems, *J. Controlled Release*, 2012, **157**, 168–182, DOI: **10.1016/j.jconrel.2011.07.031**.

11 J. Shen, J. Wolfram, M. Ferrari and H. Shen, Taking the vehicle out of drug delivery, *Mater. Today*, 2017, **20**, 95–97, DOI: **10.1016/j.mattod.2017.01.013**.

12 M. J. Mitchell, M. M. Billingsley, R. M. Haley, M. E. Wechsler, N. A. Peppas and R. Langer, Engineering precision nanoparticles for drug delivery, *Nat. Rev. Drug Discovery*, 2021, **20**, 101–124, DOI: **10.1038/s41573-020-0090-8**.

13 H. Maeda, H. Nakamura and J. Fang, The EPR effect for macromolecular drug delivery to solid tumors: Improvement of tumor uptake, lowering of systemic toxicity, and distinct tumor imaging in vivo, *Adv. Drug Delivery Rev.*, 2013, **65**, 71–79, DOI: **10.1016/j.addr.2012.10.002**.

14 V. P. Chauhan and R. K. Jain, Strategies for advancing cancer nanomedicine, *Nat. Mater.*, 2013, **12**, 958–962, DOI: **10.1038/nmat3792**.

15 V. P. Torchilin, Micellar Nanocarriers: Pharmaceutical Perspectives, *Pharm. Res.*, 2006, **24**, 1–16, DOI: 10.1007/s11095-006-9132-0.
16 M. Chatterjee, N. Jaiswal, A. Hens, N. Mahata and N. Chanda, Development of 6-Thioguanine conjugated PLGA nanoparticles through thioester bond formation: Benefits of electrospray mediated drug encapsulation and sustained release in cancer therapeutic applications, *Mater. Sci. Eng., C*, 2020, **114**, 111029, DOI: 10.1016/j.msec.2020.111029.
17 M. Chatterjee and N. Chanda, Formulation of PLGA nanocarriers: Specialized modification for cancer therapeutic applications, *Mater. Adv.*, 2022, **3**, 837–858, DOI: 10.1039/d1ma00600b.
18 M. R. Green, G. M. Manikhas, S. Orlov, B. Afanasyev, A. M. Makhson, P. Bhar and M. J. Hawkins, Abraxane®, a novel Cremophor®-free, albumin-bound particle form of paclitaxel for the treatment of advanced non-small-cell lung cancer, *Ann. Oncol.*, 2006, **17**, 1263–1268, DOI: 10.1093/annonc/mdl104.
19 A. Spada, J. Emami, J. A. Tuszynski and A. Lavasanifar, The Uniqueness of Albumin as a Carrier in Nanodrug Delivery, *Mol. Pharm.*, 2021, **18**, 1862–1894, DOI: 10.1021/acs.molpharmaceut.1c00046.
20 P. Guo, The emerging field of RNA nanotechnology, *Nat. Nanotechnol.*, 2010, **5**, 833–842, DOI: 10.1038/nnano.2010.231.
21 S. N. Baker and G. A. Baker, Luminescent Carbon Nanodots: Emergent Nanolights, *Angew. Chem., Int. Ed.*, 2010, **49**, 6726–6744, DOI: 10.1002/anie.200906623.
22 S.-J. Yu, M.-W. Kang, H.-C. Chang, K.-M. Chen and Y.-C. Yu, Bright Fluorescent Nanodiamonds: No Photobleaching and Low Cytotoxicity, *J. Am. Chem. Soc.*, 2005, **127**, 17604–17605, DOI: 10.1021/ja0567081.
23 Z. Liu, K. Chen, C. Davis, S. Sherlock, Q. Cao, X. Chen and H. Dai, Drug delivery with carbon nanotubes for in vivo cancer treatment, *Cancer Res.*, 2008, **68**, 6652–6660, DOI: 10.1158/0008-5472.CAN-08-1468.
24 L. Wang, J. Shi, H. Zhang, H. Li, Y. Gao, Z. Wang, H. Wang, L. Li, C. Zhang, C. Chen, Z. Zhang and Y. Zhang, Synergistic anticancer effect of RNAi and photothermal therapy mediated by functionalized single-walled carbon nanotubes, *Biomaterials*, 2013, **34**, 262–274, DOI: 10.1016/j.biomaterials.2012.09.037.
25 M. Nurunnabi, Z. Khatun, G. R. Reeck, D. Y. Lee and Y. Lee, Photoluminescent Graphene Nanoparticles for Cancer Phototherapy and Imaging, *ACS Appl. Mater. Interfaces*, 2014, **6**, 12413–12421, DOI: 10.1021/am504071z.
26 T. Jiang, W. Sun, Q. Zhu, N. A. Burns, S. A. Khan, R. Mo and Z. Gu, Furin-mediated sequential delivery of anticancer cytokine and small-molecule drug shuttled by graphene, *Adv. Mater.*, 2015, **27**, 1021–1028, DOI: 10.1002/adma.201404498.
27 A. Kumar, B. Mazinder Boruah and X.-J. Liang, Gold Nanoparticles: Promising Nanomaterials for the Diagnosis of Cancer and HIV/AIDS, *J. Nanomater.*, 2011, **2011**, 1–17, DOI: 10.1155/2011/202187.
28 W. Chen, S. Zhang, Y. Yu, H. Zhang and Q. He, Structural–Engineering Rationales of Gold Nanoparticles for Cancer Theranostics, *Adv. Mater.*, 2016, **28**, 8567–8585, DOI: 10.1002/adma.201602080.
29 M. Colombo, S. Carregal-Romero, M. F. Casula, L. Gutiérrez, M. P. Morales, I. B. Böhm, J. T. Heverhagen, D. Prosperi and W. J. Parak, Biological applications of magnetic nanoparticles, *Chem. Soc. Rev.*, 2012, **41**, 4306–4334, DOI: 10.1039/c2cs15337h.
30 X. Gao, Y. Cui, R. M. Levenson, L. W. K. Chung and S. Nie, In vivo cancer targeting and imaging with semiconductor quantum dots, *Nat. Biotechnol.*, 2004, **22**, 969–976, DOI: 10.1038/nbt994.
31 A. E. Nel, L. Mädler, D. Velegol, T. Xia, E. M. V. Hoek, P. Somasundaran, F. Klaessig, V. Castranova and M. Thompson, Understanding biophysicochemical interactions at the nano–bio interface, *Nat. Mater.*, 2009, **8**, 543–557, DOI: 10.1038/nmat2442.
32 R. Cai and C. Chen, The Crown and the Scepter: Roles of the Protein Corona in Nanomedicine, *Adv. Mater.*, 2019, **31**, e1805740, DOI: 10.1002/adma.201805740.
33 J. Wang, Y. Li and G. Nie, Multifunctional biomolecule nanostructures for cancer therapy, *Nat. Rev. Mater.*, 2021, **6**, 766–783, DOI: 10.1038/s41578-021-00315-x.
34 B. Kang, P. Okwieka, S. Schöttler, S. Winzen, J. Langhanki, K. Mohr, T. Opatz, V. Mailänder, K. Landfester and F. R. Wurm, Carbohydrate-Based Nanocarriers Exhibiting Specific Cell Targeting with Minimum Influence from the Protein Corona, *Angew. Chem., Int. Ed.*, 2015, **54**, 7436–7440, DOI: 10.1002/anie.201502398.
35 T. Mizuhara, K. Saha, D. F. Moyano, C. S. Kim, B. Yan, Y. K. Kim and V. M. Rotello, Acylsulfonamide-Functionalized zwitterionic gold nanoparticles for enhanced cellular uptake at tumor pH, *Angew. Chem., Int. Ed.*, 2015, **54**, 6567–6570, DOI: 10.1002/anie.201411615.
36 Q. Dai, C. Walkey and W. C. W. Chan, Polyethylene Glycol Backfilling Mitigates the Negative Impact of the Protein Corona on Nanoparticle Cell Targeting, *Angew. Chem., Int. Ed.*, 2014, **53**, 5093–5096, DOI: 10.1002/anie.201309464.
37 S. Tenzer, D. Docter, J. Kuharev, A. Musyanovych, V. Fetz, R. Hecht, F. Schlenk, D. Fischer, K. Kiouptsi, C. Reinhardt, K. Landfester, H. Schild, M. Maskos, S. K. Knauer and R. H. Stauber, Rapid formation of plasma protein corona critically affects nanoparticle pathophysiology, *Nat. Nanotechnol.*, 2013, **8**, 772–781, DOI: 10.1038/nnano.2013.181.
38 C. Corbo, R. Molinaro, F. Taraballi, N. E. Toledano Furman, K. A. Hartman, M. B. Sherman, E. De Rosa, D. K. Kirui, F. Salvatore and E. Tasciotti, Unveiling the in Vivo Protein Corona of Circulating Leukocyte-like Carriers, *ACS Nano*, 2017, **11**, 3262–3273, DOI: 10.1021/acsnano.7b00376.
39 S. Schöttler, G. Becker, S. Winzen, T. Steinbach, K. Mohr, K. Landfester, V. Mailänder and F. R. Wurm, Protein

adsorption is required for stealth effect of poly(ethylene glycol)- and poly(phosphoester)-coated nanocarriers, *Nat. Nanotechnol.*, 2016, **11**, 372–377, DOI: **10.1038/nnano.2015.330**.

40 M. Hadjidemetriou, Z. Al-Ahmady, M. Mazza, R. F. Collins, K. Dawson and K. Kostarelos, In Vivo Biomolecule Corona around Blood-Circulating, Clinically Used and Antibody-Targeted Lipid Bilayer Nanoscale Vesicles, *ACS Nano*, 2015, **9**, 8142–8156, DOI: **10.1021/acsnano.5b03300**.

41 P. C. Ke, S. Lin, W. J. Parak, T. P. Davis and F. Caruso, A Decade of the Protein Corona, *ACS Nano*, 2017, **11**, 11773–11776, DOI: **10.1021/acsnano.7b08008**.

42 A. D. Smith, Big Moment for Nanotech: Oncology Therapeutics Poised for a Leap, OncLive, 2013. **https://www.onclive.com/view/big-moment-for-nanotech-oncology-therapeutics-poised-for-a-leap**.

43 G. P. Stathopoulos, D. Antoniou, J. Dimitroulis, P. Michalopoulou, A. Bastas, K. Marosis, J. Stathopoulos, A. Provata, P. Yiamboudakis, D. Veldekis, N. Lolis, N. Georgatou, M. Toubis, C. Pappas and G. Tsoukalas, Liposomal cisplatin combined with paclitaxel versus cisplatin and paclitaxel in non-small-cell lung cancer: A randomized phase III multicenter trial, *Ann. Oncol.*, 2010, **21**, 2227–2232, DOI: **10.1093/annonc/mdq234**.

44 S. C. Gad, K. L. Sharp, C. Montgomery, J. D. Payne and G. P. Goodrich, Evaluation of the toxicity of intravenous delivery of auroshell particles (Gold-Silica Nanoshells), *Int. J. Toxicol.*, 2012, **31**, 584–594, DOI: **10.1177/1091581812465969**.

45 US National Library of Medicine. ClinicalTrials.gov, TNF-Bound Colloidal Gold in Treating Patients With Advanced Solid Tumors, 2012.

46 M. Benezra, O. Penate-Medina, P. B. Zanzonico, D. Schaer, H. Ow, A. Burns, E. DeStanchina, V. Longo, E. Herz, S. Iyer, J. Wolchok, S. M. Larson, U. Wiesner and M. S. Bradbury, Multimodal silica nanoparticles are effective cancer-targeted probes in a model of human melanoma, *J. Clin. Invest.*, 2011, **121**, 2768–2780, DOI: **10.1172/JCI45600**.

47 P. G. Tardi, N. Dos Santos, T. O. Harasym, S. A. Johnstone, N. Zisman, A. W. Tsang, D. G. Bermudes and L. D. Mayer, Drug ratio-dependent antitumor activity of irinotecan and cisplatin combinations in vitro and in vivo, *Mol. Cancer Ther.*, 2009, **8**, 2266–2275, DOI: **10.1158/1535-7163.MCT-09-0243**.

48 J. H. Fang, Y. H. Lai, T. L. Chiu, Y. Y. Chen, S. H. Hu and S. Y. Chen, Magnetic core-shell nanocapsules with dual-targeting capabilities and co-delivery of multiple drugs to treat brain gliomas, *Adv. Healthcare Mater.*, 2014, **3**, 1250–1260, DOI: **10.1002/adhm.201300598**.

49 Z. Xiao, C. Ji, J. Shi, E. M. Pridgen, J. Frieder, J. Wu and O. C. Farokhzad, DNA self-assembly of targeted near-infrared-responsive gold nanoparticles for cancer thermochemotherapy, *Angew. Chem., Int. Ed.*, 2012, **51**, 11853–11857, DOI: **10.1002/anie.201204018**.

50 V. Roy, B. R. Laplant, G. G. Gross, C. L. Bane and F. M. Palmieri, Phase II trial of weekly nab (nanoparticle albumin-bound)-paclitaxel (nab-paclitaxel) (Abraxane®) in combination with gemcitabine in patients with metastatic breast cancer (N0531), *Ann. Oncol.*, 2009, **20**, 449–453, DOI: **10.1093/annonc/mdn661**.

51 T.-W. Chen, T. J. Wardill, Y. Sun, S. R. Pulver, S. L. Renninger, A. Baohan, E. R. Schreiter, R. A. Kerr, M. B. Orger, V. Jayaraman, L. L. Looger, K. Svoboda and D. S. Kim, Ultrasensitive fluorescent proteins for imaging neuronal activity, *Nature*, 2013, **499**, 295–300, DOI: **10.1038/nature12354**.

52 K. Bolaños, M. J. Kogan and E. Araya, Capping gold nanoparticles with albumin to improve their biomedical properties, *Int. J. Nanomed.*, 2019, **14**, 6387–6406, DOI: **10.2147/IJN.S210992**.

53 S. Govindaraju, A. Rengaraj, R. Arivazhagan, Y.-S. Huh and K. Yun, Curcumin-Conjugated Gold Clusters for Bioimaging and Anticancer Applications, *Bioconjugate Chem.*, 2018, **29**, 363–370, DOI: **10.1021/acs.bioconjchem.7b00683**.

54 N. Jaiswal, S. Halder, N. Mahata and N. Chanda, Bi-Functional Gold Nanorod–Protein Conjugates with Biomimetic BSA@Folic Acid Corona for Improved Tumor Targeting and Intracellular Delivery of Therapeutic Proteins in Colon Cancer 3D Spheroids, *ACS Appl. Bio Mater.*, 2022, **5**, 1476–1488, DOI: **10.1021/acsabm.1c01216**.

55 H. Chen, B. Li, X. Ren, S. Li, Y. Ma, S. Cui and Y. Gu, Multifunctional near-infrared-emitting nano-conjugates based on gold clusters for tumor imaging and therapy, *Biomaterials*, 2012, **33**, 8461–8476, DOI: **10.1016/j.biomaterials.2012.08.034**.

56 N. Jaiswal, N. Mahata, G. Biswas and N. Chanda, Thiol responsive 6-thioguanine delivery using fluorescent gold nanoconjugate for synergistic oxidative stress amplification and chemotherapy: A combinatorial approach in cancer management, *J. Drug Delivery Sci. Technol.*, 2024, **93**, 105452, DOI: **10.1016/j.jddst.2024.105452**.

57 I. H. El-Sayed, X. Huang and M. A. El-Sayed, Surface plasmon resonance scattering and absorption of anti-EGFR antibody conjugated gold nanoparticles in cancer diagnostics: Applications in oral cancer, *Nano Lett.*, 2005, **5**, 829–834, DOI: **10.1021/nl050074e**.

58 E. L. L. Yeo, P. S. P. Thong, K. C. Soo and J. C. Y. Kah, Protein corona in drug delivery for multimodal cancer therapy: In vivo, *Nanoscale*, 2018, **10**, 2461–2472, DOI: **10.1039/c7nr08509e**.

59 W. Tang, L. Han, X. Lu, Z. Wang, F. Liu, Y. Li, S. Liu, S. Liu, R. Tian, J. Liu and B. Ding, A Nucleic Acid/Gold Nanorod-Based Nanoplatform for Targeted Gene Editing and Combined Tumor Therapy, *ACS Appl. Mater. Interfaces*, 2021, **13**, 20974–20981, DOI: **10.1021/acsami.1c02122**.

60 E. L. L. Yeo, J. U. J. Cheah, P. S. P. Thong, K. C. Soo and J. C. Y. Kah, Gold Nanorods Coated with Apolipoprotein e Protein Corona for Drug Delivery, *ACS Appl. Nano Mater.*, 2019, **2**, 6220–6229, DOI: **10.1021/acsanm.9b01196**.

61 E. L. L. Yeo, J. U. J. Cheah, B. Y. Lim, P. S. P. Thong, K. C. Soo and J. C. Y. Kah, Protein Corona around Gold Nanorods as a Drug Carrier for Multimodal Cancer Therapy, *ACS Biomater. Sci. Eng.*, 2017, **3**, 1039–1050, DOI: **10.1021/acsbiomaterials.7b00231**.

62 M. Zhang, H. S. Kim, T. Jin, J. Woo, Y. J. Piao and W. K. Moon, Near-infrared photothermal therapy using anti-EGFR-gold nanorod conjugates for triple negative breast cancer, *Oncotarget*, 2017, **8**, 86566–86575, DOI: **10.18632/oncotarget.21243**.

63 Y. Chen, X. Bian, M. Aliru, A. A. Deorukhkar, O. Ekpenyong, S. Liang, J. John, J. Ma, X. Gao, J. Schwartz, P. Singh, Y. Ye, S. Krishnan and H. Xie, Hypoxia-targeted gold nanorods for cancer photothermal therapy, *Oncotarget*, 2018, **9**, 26556–26571, DOI: **10.18632/oncotarget.25492**.

64 Y. Li, Y. Cao, L. Wei, J. Wang, M. Zhang, X. Yang, W. Wang and G. Yang, The assembly of protein-templated gold nanoclusters for enhanced fluorescence emission and multifunctional applications, *Acta Biomater.*, 2020, **101**, 436–443, DOI: **10.1016/j.actbio.2019.10.035**.

65 Y. Kong, J. Chen, F. Gao, R. Brydson, B. Johnson, G. Heath, Y. Zhang, L. Wu and D. Zhou, Near-infrared fluorescent ribonuclease-A-encapsulated gold nanoclusters: preparation, characterization, cancer targeting and imaging, *Nanoscale*, 2013, **5**, 1009–1017, DOI: **10.1039/c2nr32760k**.

66 W. Wang, Y. Kong, J. Jiang, Q. Xie, Y. Huang, G. Li, D. Wu, H. Zheng, M. Gao, S. Xu, Y. Pan, W. Li, R. Ma, M. X. Wu, X. Li, H. Zuilhof, X. Cai and R. Li, Engineering the Protein Corona Structure on Gold Nanoclusters Enables Red-Shifted Emissions in the Second Near-infrared Window for Gastrointestinal Imaging, *Angew. Chem., Int. Ed.*, 2020, **59**, 22431–22435, DOI: **10.1002/anie.202010089**.

67 L. Chen, M. Gharib, Y. Zeng, S. Roy, C. K. Nandi and I. Chakraborty, Advances in bovine serum albumin-protected gold nanoclusters: from understanding the formation mechanisms to biological applications, *Mater. Today Chem.*, 2023, **29**, 101460, DOI: **10.1016/j.mtchem.2023.101460**.

68 D. Tahir, S. Syarifuddin, E. E. M. Noor, H. Heryanto and M. A. Mohamed, Advancements in protein-based bionanocomposites for targeted and controlled drug delivery systems: A comprehensive review, *J. Drug Delivery Sci. Technol.*, 2025, **106**, 106698, DOI: **10.1016/j.jddst.2025.106698**.

69 M. Tebbe, C. Kuttner, M. Männel, A. Fery and M. Chanana, Colloidally Stable and Surfactant-Free Protein-Coated Gold Nanorods in Biological Media, *ACS Appl. Mater. Interfaces*, 2015, **7**, 5984–5991, DOI: **10.1021/acsami.5b00335**.

70 R. R. Kudarha and K. K. Sawant, Albumin based versatile multifunctional nanocarriers for cancer therapy: Fabrication, surface modification, multimodal therapeutics and imaging approaches, *Mater. Sci. Eng., C*, 2017, **81**, 607–626, DOI: **10.1016/j.msec.2017.08.004**.

71 M. S. Maleki, O. Moradi and S. Tahmasebi, Adsorption of albumin by gold nanoparticles: Equilibrium and thermodynamics studies, *Arabian J. Chem.*, 2017, **10**, S491–S502, DOI: **10.1016/j.arabjc.2012.10.009**.

72 J. Mariam, S. Sivakami and P. M. Dongre, Albumin corona on nanoparticles – a strategic approach in drug delivery, *Drug Delivery.*, 2016, **23**, 2668–2676, DOI: **10.3109/10717544.2015.1048488**.

73 J. Xie, Y. Zheng and J. Y. Ying, Protein-Directed Synthesis of Highly Fluorescent Gold Nanoclusters, *J. Am. Chem. Soc.*, 2009, **131**, 888–889, DOI: **10.1021/ja806804u**.

74 Q. Chen and Z. Liu, Albumin Carriers for Cancer Theranostics: A Conventional Platform with New Promise, *Adv. Mater.*, 2016, **28**, 10557–10566, DOI: **10.1002/adma.201600038**.

75 H. Huang, D. P. Yang, M. Liu, X. Wang, Z. Zhang, G. Zhou, W. Liu, Y. Cao, W. J. Zhang and X. Wang, pH-sensitive Au-BSA-DOX-FA nanocomposites for combined CT imaging and targeted drug delivery, *Int. J. Nanomed.*, 2017, **12**, 2829–2843, DOI: **10.2147/IJN.S128270**.

76 L. Yan, Y. Cai, B. Zheng, H. Yuan, Y. Guo, D. Xiao and M. M. F. Choi, Microwave-assisted synthesis of BSA-stabilized and HSA-protected gold nanoclusters with red emission, *J. Mater. Chem.*, 2012, **22**, 1000–1005, DOI: **10.1039/c1jm13457d**.

77 H. Liu, X. Zhang, X. Wu, L. Jiang, C. Burda and J. J. Zhu, Rapid sonochemical synthesis of highly luminescent nontoxic AuNCs and Au@AgNCs and Cu (ii) sensing, *Chem. Commun.*, 2011, **47**, 4237, DOI: **10.1039/c1cc00103e**.

78 Z. F. Pu, J. Peng, Q. L. Wen, Y. Li, J. Ling, P. Liu and Q. E. Cao, Photocatalytic synthesis of BSA-Au nanoclusters with tunable fluorescence for highly selective detection of silver ion, *Dyes Pigm.*, 2021, **193**, 109533, DOI: **10.1016/j.dyepig.2021.109533**.

79 M. A. H. Muhammed, P. K. Verma, S. K. Pal, A. Retnakumari, M. Koyakutty, S. Nair and T. Pradeep, Luminescent quantum clusters of gold in bulk by albumin-induced core etching of nanoparticles: Metal ion sensing, metal-enhanced luminescence, and biolabeling, *Chem. – Eur. J.*, 2010, **16**, 10103–10112, DOI: **10.1002/chem.201000841**.

80 F. Kratz, Albumin as a drug carrier: Design of prodrugs, drug conjugates and nanoparticles, *J. Controlled Release*, 2008, **132**, 171–183, DOI: **10.1016/j.jconrel.2008.05.010**.

81 R. Khandelia, S. Bhandari, U. N. Pan, S. S. Ghosh and A. Chattopadhyay, Gold Nanocluster Embedded Albumin Nanoparticles for Two–Photon Imaging of Cancer Cells Accompanying Drug Delivery, *Small*, 2015, **11**, 4075–4081, DOI: **10.1002/smll.201500216**.

82 A. Loureiro, N. G. Azoia, A. C. Gomes and A. Cavaco-Paulo, Albumin-Based Nanodevices as Drug Carriers, *Curr. Pharm. Des.*, 2016, **22**, 1371–1390, DOI: **10.2174/1381612822666160125114900**.

83 P. Cai, X. Zhang, M. Wang, Y.-L. Wu and X. Chen, Combinatorial Nano–Bio Interfaces, *ACS Nano*, 2018, **12**, 5078–5084, DOI: **10.1021/acsnano.8b03285**.

84 D. Rajan, R. Rajamanikandan and M. Ilanchelian, Investigating the biophysical interaction of serum albumins-gold nanorods using hybrid spectroscopic and computational approaches with the intent of enhancing cytotoxicity efficiency of targeted drug delivery, *J. Mol. Liq.*, 2023, **377**, 121541, DOI: 10.1016/j.molliq.2023.121541.

85 H. Liu, N. Pierre-Pierre and Q. Huo, Dynamic light scattering for gold nanorod size characterization and study of nanorod-protein interactions, *Gold Bull.*, 2012, **45**, 187–195, DOI: 10.1007/s13404-012-0067-4.

86 S. Pramanik, P. Banerjee, A. Sarkar and S. C. Bhattacharya, Size-dependent interaction of gold nanoparticles with transport protein: A spectroscopic study, *J. Lumin.*, 2008, **128**, 1969–1974, DOI: 10.1016/j.jlumin.2008.06.008.

87 L. Shang, Y. Wang, J. Jiang and S. Dong, PH-dependent protein conformational changes in albumin : Gold nanoparticle bioconjugates: A spectroscopic study, *Langmuir*, 2007, **23**, 2714–2721, DOI: 10.1021/la062064e.

88 M. Dockal, D. C. Carter and F. Rüker, Conformational transitions of the three recombinant domains of human serum albumin depending on pH, *J. Biol. Chem.*, 2000, **275**, 3042–3050, DOI: 10.1074/jbc.275.5.3042.

89 M. S. Strozyk, M. Chanana, I. Pastoriza-Santos, J. Pérez-Juste and L. M. Liz-Marzán, Protein/Polymer-Based Dual-Responsive Gold Nanoparticles with pH-Dependent Thermal Sensitivity, *Adv. Funct. Mater.*, 2012, **22**, 1436–1444, DOI: 10.1002/adfm.201102471.

90 V. D. Jaiswal, D. S. Pangam and P. M. Dongre, Biophysical study of cisplatin loaded albumin-gold nanoparticle and its interaction with glycans of gp60 receptor, *Int. J. Biol. Macromol.*, 2023, **231**, 123368, DOI: 10.1016/j.ijbiomac.2023.123368.

91 W. Zhong, M. Wen, J. Xu, H. Wang, L.-L. Tan and L. Shang, Simultaneous regulation of optical properties and cellular behaviors of gold nanoclusters by pre-engineering the biotemplates, *Chem. Commun.*, 2020, **56**, 11414–11417, DOI: 10.1039/D0CC04039H.

92 A. Bunker and T. Róg, Mechanistic Understanding From Molecular Dynamics Simulation in Pharmaceutical Research 1: Drug Delivery, *Front. Mol. Biosci.*, 2020, **7**, 604770, DOI: 10.3389/fmolb.2020.604770.

93 S. Kaumbekova, N. Sakaguchi, D. Shah and M. Umezawa, Effect of Gold Nanoparticles on the Conformation of Bovine Serum Albumin: Insights from CD Spectroscopic Analysis and Molecular Dynamics Simulations, *ACS Omega*, 2024, **9**, 49283–49292.

94 F. Ramezani, M. Amanlou and H. Rafii-Tabar, Gold nanoparticle shape effects on human serum albumin corona interface: A molecular dynamic study, *J. Nanopart. Res.*, 2014, **16**, 2512, DOI: 10.1007/s11051-014-2512-1.

95 F. Ramezani and H. Rafii-Tabar, An in-depth view of human serum albumin corona on gold nanoparticles, *Mol. BioSyst.*, 2015, **11**, 454–462, DOI: 10.1039/c4mb00591k.

96 Y. Wu, M. R. K. Ali, K. Chen, N. Fang and M. A. El-Sayed, Gold nanoparticles in biological optical imaging, *Nano Today*, 2019, **24**, 120–140, DOI: 10.1016/j.nantod.2018.12.006.

97 K. L. Kelly, E. Coronado, L. L. Zhao and G. C. Schatz, The Optical Properties of Metal Nanoparticles: The Influence of Size, Shape, and Dielectric Environment, *J. Phys. Chem. B*, 2003, **107**, 668–677, DOI: 10.1021/jp026731y.

98 X. Ren, M. Li, M. Chen, Y. Dai, T. Shi and Y. L. Zhao, Characterization of protein-conjugating kinetics based on localized surface plasmon resonance of the gold nanoparticle, *Spectrosc. Lett.*, 2016, **49**, 434–443, DOI: 10.1080/00387010.2016.1192554.

99 S. E. Skrabalak, J. Chen, Y. Sun, X. Lu, L. Au, C. M. Cobley and Y. Xia, Gold Nanocages: Synthesis, Properties, and Applications, *Acc. Chem. Res.*, 2008, **41**, 1587–1595, DOI: 10.1021/ar800018v.

100 X. Wen, P. Yu, Y.-R. Toh and J. Tang, Structure-Correlated Dual Fluorescent Bands in BSA-Protected Au 25 Nanoclusters, *J. Phys. Chem. C*, 2012, **116**, 11830–11836, DOI: 10.1021/jp303530h.

101 K. T. Chuang and Y. W. Lin, Microwave-Assisted Formation of Gold Nanoclusters Capped in Bovine Serum Albumin and Exhibiting Red or Blue Emission, *J. Phys. Chem. C*, 2017, **121**, 26997–27003, DOI: 10.1021/acs.jpcc.7b09349.

102 X. L. Cao, H. W. Li, Y. Yue and Y. Wu, PH-Induced, conformational changes of BSA in fluorescent AuNCs@BSA and its effects on NCs emission, *Vib. Spectrosc.*, 2013, **65**, 186–192, DOI: 10.1016/j.vibspec.2013.01.004.

103 X. Le Guével, B. Hötzer, G. Jung, K. Hollemeyer, V. Trouillet and M. Schneider, Formation of fluorescent metal (Au, Ag) nanoclusters capped in bovine serum albumin followed by fluorescence and spectroscopy, *J. Phys. Chem. C*, 2011, **115**, 10955–10963, DOI: 10.1021/jp111820b.

104 S. Raut, R. Chib, R. Rich, D. Shumilov, Z. Gryczynski and I. Gryczynski, Polarization properties of fluorescent BSA protected Au25 nanoclusters, *Nanoscale*, 2013, **5**, 3441–3446, DOI: 10.1039/c3nr34152f.

105 A. Retnakumari, S. Setua, D. Menon, P. Ravindran, H. Muhammed, T. Pradeep, S. Nair and M. Koyakutty, Molecular-receptor-specific, non-toxic, near-infrared-emitting Au cluster-protein nanoconjugates for targeted cancer imaging, *Nanotechnology*, 2010, **21**, 055103, DOI: 10.1088/0957-4484/21/5/055103.

106 L. Crawford, M. Wyatt, J. Bryers and B. Ratner, Biocompatibility Evolves: Phenomenology to Toxicology to Regeneration, *Adv. Healthcare Mater.*, 2021, **10**, 2002153, DOI: 10.1002/adhm.202002153.

107 A. K. Barui, J. Y. Oh, B. Jana, C. Kim and J. Ryu, Cancer–Targeted Nanomedicine: Overcoming the Barrier of the Protein Corona, *Adv. Ther.*, 2020, **3**, 1900124, DOI: 10.1002/adtp.201900124.

108 P. Khullar, V. Singh, A. Mahal, P. N. Dave, S. Thakur, G. Kaur, J. Singh, S. Singh Kamboj and M. Singh Bakshi, Bovine Serum Albumin Bioconjugated Gold Nanoparticles: Synthesis, Hemolysis, and Cytotoxicity

toward Cancer Cell Lines, *J. Phys. Chem. C*, 2012, **116**, 8834–8843, DOI: 10.1021/jp300585d.

109 M. Hameed, S. Panicker, S. H. Abdallah, A. A. Khan, C. Han, M. M. Chehimi and A. A. Mohamed, Protein-Coated Aryl Modified Gold Nanoparticles for Cellular Uptake Study by Osteosarcoma Cancer Cells, *Langmuir*, 2020, **36**, 11765–11775, DOI: 10.1021/acs.langmuir.0c01443.

110 S. Sasidharan, D. Bahadur and R. Srivastava, Albumin stabilized gold nanostars: a biocompatible nanoplatform for SERS, CT imaging and photothermal therapy of cancer, *RSC Adv.*, 2016, **6**, 84025–84034, DOI: 10.1039/C6RA11405A.

111 L. Mocan, C. Matea, F. A. Tabaran, O. Mosteanu, T. Pop, C. Puia, L. Agoston-Coldea, G. Zaharie, T. Mocan, A. D. Buzoianu and C. Iancu, Selective ex vivo photothermal nano-therapy of solid liver tumors mediated by albumin conjugated gold nanoparticles, *Biomaterials*, 2017, **119**, 33–42, DOI: 10.1016/j.biomaterials.2016.12.009.

112 M. Schäffler, F. Sousa, A. Wenk, L. Sitia, S. Hirn, C. Schleh, N. Haberl, M. Violatto, M. Canovi, P. Andreozzi, M. Salmona, P. Bigini, W. G. Kreyling and S. Krol, Blood protein coating of gold nanoparticles as potential tool for organ targeting, *Biomaterials*, 2014, **35**, 3455–3466, DOI: 10.1016/j.biomaterials.2013.12.100.

113 T. Li, Y. Wang, M. Wang, L. Zheng, W. Dai, C. Jiao, Z. Song, Y. Ma, Y. Ding, Z. Zhang, F. Yang and X. He, Impact of Albumin Pre-Coating on Gold Nanoparticles Uptake at Single-Cell Level, *Nanomaterials*, 2022, **12**, 749, DOI: 10.3390/nano12050749.

114 L. Scheetz, K. S. Park, Q. Li, P. R. Lowenstein, M. G. Castro, A. Schwendeman and J. J. Moon, Engineering patient-specific cancer immunotherapies, *Nat. Biomed. Eng.*, 2019, **3**, 768–782, DOI: 10.1038/s41551-019-0436-x.

115 Y. Matsumura and H. Maeda, A New Concept for Macromolecular Therapeutics in Cancer Chemotherapy: Mechanism of Tumoritropic Accumulation of Proteins and the Antitumor Agent Smancs, *Cancer Res.*, 1986, **46**, 6387–6392.

116 D. Rosenblum, N. Joshi, W. Tao, J. M. Karp and D. Peer, Progress and challenges towards targeted delivery of cancer therapeutics, *Nat. Commun.*, 2018, **9**, 1410, DOI: 10.1038/s41467-018-03705-y.

117 H.-T. Chiu, C.-H. Chen, M.-L. Li, C.-K. Su, Y.-C. Sun, C.-S. Chiang and Y.-F. Huang, Bioprosthesis of Core–Shell Gold Nanorod/Serum Albumin Nanoimitation: A Half-Native and Half-Artificial Nanohybrid for Cancer Theranostics, *Chem. Mater.*, 2018, **30**, 729–747, DOI: 10.1021/acs.chemmater.7b04127.

118 F. Ren, S. Bhana, D. D. Norman, J. Johnson, L. Xu, D. L. Baker, A. L. Parrill and X. Huang, Gold nanorods carrying paclitaxel for photothermal-chemotherapy of cancer, *Bioconjugate Chem.*, 2013, **24**, 376–386, DOI: 10.1021/bc300442d.

119 K. Langer, M. G. Anhorn, I. Steinhauser, S. Dreis, D. Celebi, N. Schrickel, S. Faust and V. Vogel, Human serum albumin (HSA) nanoparticles: Reproducibility of preparation process and kinetics of enzymatic degradation, *Int. J. Pharm.*, 2008, **347**, 109–117, DOI: 10.1016/j.ijpharm.2007.06.028.

120 D. V. Peralta, Z. Heidari, S. Dash and M. A. Tarr, Hybrid paclitaxel and gold nanorod-loaded human serum albumin nanoparticles for simultaneous chemotherapeutic and photothermal therapy on 4T1 breast cancer cells, *ACS Appl. Mater. Interfaces*, 2015, **7**, 7101–7111, DOI: 10.1021/acsami.5b00858.

121 L. Ouyang, R. Shaik, R. Xu, G. Zhang and J. Zhe, Mapping surface charge distribution of single–cell via charged nanoparticle, *Cells*, 2021, **10**, 1519, DOI: 10.3390/cells10061519.

122 Z. Wang, L. Chen, Z. Chu, C. Huang, Y. Huang and N. Jia, Gemcitabine-loaded gold nanospheres mediated by albumin for enhanced anti-tumor activity combining with CT imaging, *Mater. Sci. Eng., C*, 2018, **89**, 106–118, DOI: 10.1016/j.msec.2018.03.025.

123 L. Dong, M. Li, S. Zhang, J. Li, G. Shen, Y. Tu, J. Zhu and J. Tao, Cytotoxicity of BSA-stabilized gold nanoclusters: In vitro and in vivo study, *Small*, 2015, **11**, 2571–2581, DOI: 10.1002/smll.201403481.

124 C. Fu, C. Ding, X. Sun and A. Fu, Curcumin nanocapsules stabilized by bovine serum albumin-capped gold nanoclusters (BSA-AuNCs) for drug delivery and theranosis, *Mater. Sci. Eng., C*, 2018, **87**, 149–154, DOI: 10.1016/j.msec.2017.12.028.

125 S. Govindaraju, A. Roshini, M. H. Lee and K. Yun, Kaempferol conjugated gold nanoclusters enabled efficient for anticancer therapeutics to A549 lung cancer cells, *Int. J. Nanomed.*, 2019, **14**, 5147–5157, DOI: 10.2147/IJN.S209773.

126 A. Latorre, A. Latorre, M. Castellanos, C. R. Diaz, A. Lazaro-Carrillo, T. Aguado, M. Lecea, S. Romero-Pérez, M. Calero, J. M. Sanchez-Puelles, Á. Villanueva and Á. Somoza, Multifunctional albumin-stabilized gold nanoclusters for the reduction of cancer stem cells, *Cancers*, 2019, **11**, 969, DOI: 10.3390/cancers11070969.

127 B. A. Lakshmi and S. Kim, Quercetin mediated gold nanoclusters explored as a dual functional nanomaterial in anticancer and bio-imaging disciplines, *Colloids Surf., B*, 2019, **178**, 230–237, DOI: 10.1016/j.colsurfb.2019.02.054.

128 G. Gao, W. Zhou, X. Jiang and J. Ma, Bovine serum albumin and folic acid-modified aurum nanoparticles loaded with paclitaxel and curcumin enhance radiotherapy sensitization for esophageal cancer, *Int. J. Radiat. Biol.*, 2024, **100**, 411–419, DOI: 10.1080/09553002.2023.2281524.

129 S. Rana, A. Bajaj, R. Mout and V. M. Rotello, Monolayer coated gold nanoparticles for delivery applications, *Adv. Drug Delivery Rev.*, 2012, **64**, 200–216, DOI: 10.1016/j.addr.2011.08.006.

130 K. M. Camacho, S. Kumar, S. Menegatti, D. R. Vogus, A. C. Anselmo and S. Mitragotri, Synergistic antitumor activity of camptothecin-doxorubicin combinations and their conjugates with hyaluronic acid, *J. Controlled Release*, 2015, **210**, 198–207, DOI: **10.1016/j.jconrel.2015.04.031**.

131 K. A. Whitehead, R. Langer and D. G. Anderson, Knocking down barriers: advances in siRNA delivery, *Nat. Rev. Drug Discovery*, 2009, **8**, 129–138, DOI: **10.1038/nrd2742**.

132 Q. Ji, H. Zhu, Y. Qin, R. Zhang, L. Wang, E. Zhang, X. Zhou and R. Meng, GP60 and SPARC as albumin receptors: key targeted sites for the delivery of antitumor drugs, *Front. Pharmacol.*, 2024, **15**, 1329636, DOI: **10.3389/fphar.2024.1329636**.

133 F. Zhou, B. Feng, H. Yu, D. Wang, T. Wang, J. Liu, Q. Meng, S. Wang, P. Zhang, Z. Zhang and Y. Li, Cisplatin prodrug-conjugated gold nanocluster for fluorescence imaging and targeted therapy of the breast cancer, *Theranostics*, 2016, **6**, 679–687, DOI: **10.7150/thno.14556**.

134 D. B. Shennan, J. Thomson, I. F. Gow, M. T. Travers and M. C. Barber, l-Leucine transport in human breast cancer cells (MCF-7 and MDA-MB-231): kinetics, regulation by estrogen and molecular identity of the transporter, *Biochim. Biophys. Acta, Biomembr.*, 2004, **1664**, 206–216, DOI: **10.1016/j.bbamem.2004.05.008**.

135 J. H. Choi, H. J. Hwang, S. W. Shin, J. W. Choi, S. H. Um and B. K. Oh, A novel albumin nanocomplex containing both small interfering RNA and gold nanorods for synergetic anticancer therapy, *Nanoscale*, 2015, **7**, 9229–9237, DOI: **10.1039/c5nr00211g**.

136 G. A. Hobbs and C. J. Der, Binge Drinking: Macropinocytosis Promotes Tumorigenic Growth of RAS-Mutant Cancers, *Trends Biochem. Sci.*, 2020, **45**, 459–461, DOI: **10.1016/j.tibs.2020.02.009**.

137 A. R. Fernandes, J. Jesus, P. Martins, S. Figueiredo, D. Rosa, L. M. R. D. R. S. Martins, M. L. Corvo, M. C. Carvalheiro, P. M. Costa and P. V. Baptista, Multifunctional gold-nanoparticles: A nanovectorization tool for the targeted delivery of novel chemotherapeutic agents, *J. Controlled Release*, 2017, **245**, 52–61, DOI: **10.1016/j.jconrel.2016.11.021**.

138 E. Achilli, C. Y. Flores, C. F. Temprana, S. V. del Alonso, M. Radrizzani and M. Grasselli, Enhanced gold nanoparticle-tumor cell recognition by albumin multilayer coating, *OpenNano*, 2022, **6**, 100033, DOI: **10.1016/j.onano.2021.100033**.

139 A. G. Tkachenko, H. Xie, D. Coleman, W. Glomm, J. Ryan, M. F. Anderson, S. Franzen and D. L. Feldheim, Multifunctional gold nanoparticle-peptide complexes for nuclear targeting, *J. Am. Chem. Soc.*, 2003, **125**, 4700–4701, DOI: **10.1021/ja0296935**.

140 A. G. Tkachenko, H. Xie, Y. Liu, D. Coleman, J. Ryan, W. R. Glomm, M. K. Shipton, S. Franzen and D. L. Feldheim, Cellular trajectories of peptide-modified gold particle complexes: Comparison of nuclear localization signals and peptide transduction domains, *Bioconjugate Chem.*, 2004, **15**, 482–490, DOI: **10.1021/bc034189q**.

141 B. Leader, Q. J. Baca and D. E. Golan, Protein therapeutics: a summary and pharmacological classification, *Nat. Rev. Drug Discovery*, 2008, **7**, 21–39, DOI: **10.1038/nrd2399**.

142 Z. Gu, A. Biswas, M. Zhao and Y. Tang, Tailoring nanocarriers for intracellular protein delivery, *Chem. Soc. Rev.*, 2011, **40**, 3638, DOI: **10.1039/c0cs00227e**.

143 R. Khandelia, A. Jaiswal, S. S. Ghosh and A. Chattopadhyay, Gold Nanoparticle–Protein Agglomerates as Versatile Nanocarriers for Drug Delivery, *Small*, 2013, **9**, 3494–3505, DOI: **10.1002/smll.201203095**.

144 H. Zafar, J. Zhang, F. Raza, X. Pan, Z. Hu, H. Feng and Q. Shen, Biomimetic gold nanocages incorporating copper-human serum albumin for tumor immunotherapy via cuproptosis-lactate regulation, *J. Controlled Release*, 2024, **372**, 446–466.

145 D. Zhang, P. Liu, X. Qin, L. Cheng, F. Wang, X. Xiong, C. Huang and Z. Zhang, HSA-templated self-generation of gold nanoparticles for tumor vaccine delivery and combinational therapy, *J. Mater. Chem. B*, 2022, **10**, 8750–8759, DOI: **10.1039/d2tb01483a**.

146 W. Zhang, J. Ye, Y. Zhang, Q. Li, X. Dong, H. Jiang and X. Wang, One-step facile synthesis of fluorescent gold nanoclusters for rapid bio-imaging of cancer cells and small animals, *RSC Adv.*, 2015, **5**, 63821–63826, DOI: **10.1039/C5RA11321K**.

147 Y. Xiao, Z. Wu, Q. Yao and J. Xie, Luminescent metal nanoclusters: Biosensing strategies and bioimaging applications, *Aggregate*, 2021, **2**, 114–132, DOI: **10.1002/agt2.11**.

148 P. Zhang, X. X. Yang, Y. Wang, N. W. Zhao, Z. H. Xiong and C. Z. Huang, Rapid synthesis of highly luminescent and stable Au20 nanoclusters for active tumor-targeted imaging in vitro and in vivo, *Nanoscale*, 2014, **6**, 2261–2269, DOI: **10.1039/c3nr05269a**.

149 A. Yadav, N. C. Verma, C. Rao, P. M. Mishra, A. Jaiswal and C. K. Nandi, Bovine Serum Albumin-Conjugated Red Emissive Gold Nanocluster as a Fluorescent Nanoprobe for Super-resolution Microscopy, *J. Phys. Chem. Lett.*, 2020, **11**, 5741–5748, DOI: **10.1021/acs.jpclett.0c01354**.

150 X. Wu, X. He, K. Wang, C. Xie, B. Zhou and Z. Qing, Ultrasmall near-infrared gold nanoclusters for tumor fluorescence imaging in vivo, *Nanoscale*, 2010, **2**, 2244–2249, DOI: **10.1039/c0nr00359j**.

151 Y. Wang, C. Xu, J. Zhai, F. Gao, R. Liu, L. Gao, Y. Zhao, Z. Chai and X. Gao, Label-free Au cluster used for in vivo 2D and 3D computed tomography of murine kidneys, *Anal. Chem.*, 2015, **87**, 343–345, DOI: **10.1021/ac503887c**.

152 W. Zhou, Y. Cao, D. Sui, W. Guan, C. Lu and J. Xie, Ultrastable BSA-capped gold nanoclusters with a polymer-like shielding layer against reactive oxygen species in living cells, *Nanoscale*, 2016, **8**, 9614–9620, DOI: **10.1039/c6nr02178f**.

153 X. Le Guével, B. Hötzer, G. Jung and M. Schneider, NIR-emitting fluorescent gold nanoclusters doped in silica

nanoparticles, *J. Mater. Chem.*, 2011, **21**, 2974, DOI: 10.1039/c0jm02660c.

154 Y. Wang, J. Chen and J. Irudayaraj, Nuclear targeting dynamics of gold nanoclusters for enhanced therapy of HER2 + breast cancer, *ACS Nano*, 2011, **5**, 9718–9725, DOI: 10.1021/nn2032177.

155 W. Gu, Q. Zhang, T. Zhang, Y. Li, J. Xiang, R. Peng and J. Liu, Hybrid polymeric nano-capsules loaded with gold nanoclusters and indocyanine green for dual-modal imaging and photothermal therapy, *J. Mater. Chem. B*, 2016, **4**, 910–919, DOI: 10.1039/c5tb01619c.

156 H. Shi, Z. Wang, C. Huang, X. Gu, T. Jia, A. Zhang, Z. Wu, L. Zhu, X. Luo, X. Zhao, N. Jia and F. Miao, A Functional CT Contrast Agent for In Vivo Imaging of Tumor Hypoxia, *Small*, 2016, **12**, 3995–4006, DOI: 10.1002/smll.201601029.

157 X. Chen, H. Zhu, X. Huang, P. Wang, F. Zhang, W. Li, G. Chen and B. Chen, Novel iodinated gold nanoclusters for precise diagnosis of thyroid cancer, *Nanoscale*, 2017, **9**, 2219–2231, DOI: 10.1039/c6nr07656d.

158 S. K. Sun, L. X. Dong, Y. Cao, H. R. Sun and X. P. Yan, Fabrication of multifunctional Gd_2O3/Au hybrid nanoprobe via a one-step approach for near-infrared fluorescence and magnetic resonance multimodal imaging in vivo, *Anal. Chem.*, 2013, **85**, 8436–8441, DOI: 10.1021/ac401879y.

159 D. H. Hu, Z. H. Sheng, P. F. Zhang, D. Z. Yang, S. H. Liu, P. Gong, D. Y. Gao, S. T. Fang, Y. F. Ma and L. T. Cai, Hybrid gold-gadolinium nanoclusters for tumor-targeted NIRF/CT/MRI triple-modal imaging in vivo, *Nanoscale*, 2013, **5**, 1624–1628, DOI: 10.1039/c2nr33543c.

160 C. Xu, Y. Wang, C. Zhang, Y. Jia, Y. Luo and X. Gao, AuGd integrated nanoprobes for optical/MRI/CT triple-modal in vivo tumor imaging, *Nanoscale*, 2017, **9**, 4620–4628, DOI: 10.1039/c7nr01064h.

161 M. Hauser, M. Wojcik, D. Kim, M. Mahmoudi, W. Li and K. Xu, Correlative Super-Resolution Microscopy: New Dimensions and New Opportunities, *Chem. Rev.*, 2017, **117**, 7428–7456, DOI: 10.1021/acs.chemrev.6b00604.

162 D. Hanahan and R. A. Weinberg, The Hallmarks of Cancer, *Cell*, 2000, **100**, 57–70, DOI: 10.1016/S0092-8674(00)81683-9.

163 D. Hanahan, Hallmarks of Cancer: New Dimensions, *Cancer Discovery*, 2022, **12**, 31–46, DOI: 10.1158/2159-8290.CD-21-1059.

164 B. Nath, A. P. Bidkar, V. Kumar, A. Dalal, M. K. Jolly, S. S. Ghosh and G. Biswas, Deciphering Hydrodynamic and Drug-Resistant Behaviors of Metastatic EMT Breast Cancer Cells Moving in a Constricted Microcapillary, *J. Clin. Med.*, 2019, **8**, 1194, DOI: 10.3390/jcm8081194.

165 N. Jaiswal, A. Hens, M. Chatterjee, N. Mahata and N. Chanda, Ethylenediamine assisted functionalization of self-organized poly (d, l-lactide-co-glycolide) patterned surface to enhance cancer cell isolation, *J. Colloid Interface Sci.*, 2019, **534**, 122–130, DOI: 10.1016/j.jcis.2018.08.111.

166 S. Li, K. Wang, S. Hao, F. Dang, Z. Q. Zhang and J. Zhang, Antifouling Gold-Inlaid BSA Coating for the Highly Efficient Capture of Circulating Tumor Cells, *Anal. Chem.*, 2022, **94**, 6754–6759, DOI: 10.1021/acs.analchem.2c00246.

167 M. Zhao, D. Mi, B. E. Ferdows, Y. Li, R. Wang, J. Li, D. Patel, N. Kong, S. Shi and W. Tao, State-of-the-art nanotechnologies for the detection, recovery, analysis and elimination of liquid biopsy components in cancer, *Nano Today*, 2022, **42**, 101361, DOI: 10.1016/j.nantod.2021.101361.

168 X. Wu, Y. Xia, Y. Huang, J. Li, H. Ruan, T. Chen, L. Luo, Z. Shen and A. Wu, Improved SERS-Active Nanoparticles with Various Shapes for CTC Detection without Enrichment Process with Supersensitivity and High Specificity, *ACS Appl. Mater. Interfaces*, 2016, **8**, 19928–19938, DOI: 10.1021/acsami.6b07205.

169 T. Wu, K. Chen, W. Lai, H. Zhou, X. Wen, H. F. Chan, M. Li, H. Wang and Y. Tao, Bovine serum albumin-gold nanoclusters protein corona stabilized polystyrene nanoparticles as dual-color fluorescent nanoprobes for breast cancer detection, *Biosens. Bioelectron.*, 2022, **215**, 114575, DOI: 10.1016/j.bios.2022.114575.

170 P. Nath, M. Chatterjee and N. Chanda, Dithiothreitol-Facilitated Synthesis of Bovine Serum Albumin–Gold Nanoclusters for Pb(II) Ion Detection on Paper Substrates and in Live Cells, *ACS Appl. Nano Mater.*, 2018, **1**, 5108–5118, DOI: 10.1021/acsanm.8b01191.

171 N. Priyadarshni, P. Nath, N. Nagahanumaiah and N. Chanda, DMSA-Functionalized Gold Nanorod on Paper for Colorimetric Detection and Estimation of Arsenic (III and V) Contamination in Groundwater, *ACS Sustainable Chem. Eng.*, 2018, **6**, 6264–6272, DOI: 10.1021/acssuschemeng.8b00068.

172 M. Yu, S. Stott, M. Toner, S. Maheswaran and D. A. Haber, Circulating tumor cells: approaches to isolation and characterization, *J. Cell Biol.*, 2011, **192**, 373–382, DOI: 10.1083/jcb.201010021.

173 A. Cheung, H. J. Bax, D. H. Josephs, K. M. Ilieva, G. Pellizzari, J. Opzoomer, J. Bloomfield, M. Fittall, A. Grigoriadis, M. Figini, S. Canevari, J. F. Spicer, A. N. Tutt and S. N. Karagiannis, Targeting folate receptor alpha for cancer treatment, *Oncotarget*, 2016, **7**, 52553–52574, DOI: 10.18632/oncotarget.9651.

174 Z. Deng, S. Wu, Y. Wang and D. Shi, Circulating tumor cell isolation for cancer diagnosis and prognosis, *EBioMedicine*, 2022, **83**, 104237, DOI: 10.1016/j.ebiom.2022.104237.

175 S. Nagrath, L. V. Sequist, S. Maheswaran, D. W. Bell, D. Irimia, L. Ulkus, M. R. Smith, E. L. Kwak, S. Digumarthy, A. Muzikansky, P. Ryan, U. J. Balis, R. G. Tompkins, D. A. Haber and M. Toner, Isolation of rare circulating tumour cells in cancer patients by microchip technology, *Nature*, 2007, **450**, 1235–1239, DOI: 10.1038/nature06385.

176 A. D. Waldman, J. M. Fritz and M. J. Lenardo, A guide to cancer immunotherapy: from T cell basic science to clinical practice, *Nat. Rev. Immunol.*, 2020, **20**(11), 651–668, DOI: 10.1038/s41577-020-0306-5.